Visible light communication CMOS image sensor for automotive applications

Kristian Geli Nilsen

Thesis submitted for the degree of
Master in Nanoelectronics
60 credits

Department of Informatics
Faculty of mathematics and natural sciences

UNIVERSITY OF OSLO

Spring 2019

Visible light communication CMOS image sensor for automotive applications

Kristian Geli Nilsen

Visible light communication CMOS image sensor for automotive applications

http://www.duo.uio.no/

Printed: Reprosentralen, University of Oslo

Abstract

In this project, an image sensor designed to receive modulated light was designed and produced. Earlier, an image sensor consisting of alternating pixel topologies has been produced and tested. However, using a single pixel topology may have its advantages. In this project, a single pixel topology image sensor for visible light communication and image capturing is explored. A PCB to mount and interface the image sensor to an FPGA has been designed. The analysis of the circuits data bandwidth and performance is provided based on simulation results. However, due to a 6-month production delay at AMS, the image sensor has not been delivered, in time for measurements.

Preface

This was submitted as my master thesis for my master's degree at the University of Oslo. Unfortunately, due to the production delay, the chip was not delivered in time, which caused this thesis to be short and miss pages about measurements and results. Working on this project and reading literature about visible light communication has made me interested in this field. When the chip returns, I will do the measurements and finish this project. I want to thank my supervisor Philipp Hafliger and the members of the bi-weekly meeting with the supervising group: Mozhdeh Nematzadeh, Behnam Samadpoor Rikan, and Joar Martin Østby. Thanks to Marius Lillestøl for showing me how to enable hidden layers.

Contents

List of Figures

List of Tables

Part I

Introduction

g

Chapter 1

Background

1.1 Visible light communication

Today, most of the new light sources are light emitting diodes (LEDs). LEDs have the advantages over traditional light sources such as incandescent and fluorescent lamps that it can be modulated at a high frequency, low power consumption, longer lifespan, high radiation power, more robust and small size [1]. LEDs can be found almost anywhere there is light, from phone displays, TVs, street lights, traffic lights, vehicle taillights and other lights used to capture the attention of the eye. The widespread use of LEDs and its fast switching capability gives it an attractive use for communication. The LEDs ability for fast switching gives LEDs the capability to transmit data efficiently on existing infrastructure [2].

Visible light communication (VLC) is optical wireless communication in the visible light spectrum. The VLC spectrum is defined as wavelengths from 380nm to 780nm in the electromagnetic spectrum, which corresponds to the bandwidth of 384Thz to 788Thz. The VLC spectrum is significantly broader than the radio frequency (RF) spectrum, and it is not regulated and crowded [3]. VLC offers a high-quality and secure link between the transmitter and receiver, because of a direct line of sight (LOS). Additionally, when an image sensor is used as a receiver, the signal source can be spatially separated and provide a high signal to noise ratio (SNR) with the possibility to receive from multiple transmitters. By having a LOS communication link, problems that RF have with reflections, distortions, and interference are negated.

One application of VLC is indoor localization [3]. Indoor localization can be used to provide good accuracy positioning in supermarkets, malls, and airports. This can also be used for indoor navigation both for people and robots. Internet of things (IoT) devices, are going to be more common and will be found almost everywhere both in the home and outside. One way to connect all these devices is to use VLC. Intelligent transport systems (ITS) is communication between vehicles to vehicles and vehicles to road infrastructure, and can also be done with VLC, more on this in chapter 1.2. VLC can be used in restricted areas such as aircraft, spaceships, and hospitals. These places have instruments and equipment which are

vulnerable to RF interference. These instruments and equipment should not be exposed to unnecessary RF, as it can cause interference with aircraft communication and navigation. Radio interference is critical in aircraft because the communication with air traffic control is over the radio, and any interference should be avoided [4][5]. In hospitals, instruments that are sensitive to electromagnetic noise can be affected by RF signals which can affect the quality of measurements. Wireless local area network (WLAN) can be realized using VLC. VLC WLAN can be used in aircraft cabins to provide internet access to the passengers, and this can be done by modulating the reading light or cabin light to provide a downlink for computers and smartphones.

Information is transmitted by LEDs using modulation. Different types of modulation have been used and developed [5]. The standard type of modulation is on-off keying, which is to turn the LED on and off to transmit a signal. One way to regulate the brightness of an LED is by pulse width modulation (PWM). PWM is a modulation technique used to reduce the power usage of LEDs, and for dimming, this is done by turning on the LED for a given pulse width then turn it off. The human eyes perceive the modulated light as lower brightness. The frequency of the transmission modulation must be high enough not to be noticeable for human vision as flickering. The modulation type needs to prevent flicker mitigation and have dimming support. It should also prevent long chains of "off" signal because this and flickering can cause strain on eyes.

IEEE has defined a standard for VLC, IEEE 802.15.7. This standard has flicker mitigation and dimming support. It also has support for indoor and outdoor communication from 11.67kbit/s to 96.6Mbit/s. However, this standard does not define any specific information about the vehicle to vehicle implementation. A revision has been made to the IEEE 802.15.7 to support additional receivers and applications. The new revision, IEEE 802.15.7r1 supports vehicle-to-vehicle (V2V) VLC and vehicle-to-infrastructure (V2I) VLC, it also adds support for using image sensors as VLC receiver. A comparison between VLC and RF characteristics are shown in Table 1.1.

Property	**VLC**	**RF**
Bandwidth	Unlimited, 380nm to 780nm	Regulatory, BW limited
EMI	No	High
Line of sight	Yes	No
Standard	IEEE 802.15.7/r1	Matured
Visibility (Security)	Yes	No
Power Consumption	Relatively low	Medium
Distance	Short (long with laser)	Medium

Table 1.1: Comparing VLC to RF [6].

1.2 Intelligent transport system

In this project, the main application is for automotive use. The two main applications are V2V-VLC and V2I-VLC. The future of transportation is going towards fully autonomous. To achieve fully autonomous driving vehicles need to be aware of everything in its surrounding. Fully autonomous vehicles need to be able to communicate with other vehicles and infrastructure. This can be realized by exploiting a combination of VLC and dedicated short-range communication (DSRC) to create an image of its surroundings. With VLC a vehicle can get information from the vehicle in front, it can send information to the vehicle behind, and even receive information from traffic lights in an intersection as shown in Figure 1.1.

DSRC is a great complementary solution for VLC. With the use of DSRC vehicles can extend its awareness beyond the line of sight. A vehicle can communicate with a vehicle around a corner, or a vehicle behind another vehicle to get a better awareness of vehicles out of sight.

Information about the road ahead can be transmitted to vehicles using LED signs and traffic lights. If there is a narrowing in the road, construction work, temporary detours, and other dangers, vehicles can get information about this from infrastructure or cars ahead which can relay information backwards through vehicle taillights. With this information, vehicles can then adapt to the situation and prevent traffic congestion.

According to the World Health Organization [7], 1.35 million lives are lost in traffic-related incidents each year. Additionally, 20 to 50 million people suffer from non-fatal injuries. For people aged between 15 and 29 years, traffic accidents are the leading cause of death. These deaths and injuries cost people and nations billions worth of dollars. The leading cause of traffic accidents is human errors, which can be speeding, driving under the influence of alcohol or drugs, distracted by phone use and not wearing seatbelts.

When a vehicle has communication with other vehicles in its surroundings, it can improve safety significantly, perhaps make it impossible to crash. The vehicle has an awareness of its surroundings and can calculate that it will crash if it does not divert or interrupt. This feature, alone could potentially save thousands of lives, and save billions of dollar every year across the world. Traffic flow can be increased dramatically, by having all vehicles connected. For example, an intersection, instead of one vehicle pulling away at the time, every vehicle in the line can start driving synchronously. The traffic lights can detect a car which will run through a red light, then send information to vehicles that are about to cross the intersection that a vehicle is about to run a through a red light and stop them from entering the intersection and reduce the amount of side impact collisions in an intersection. Advanced cruise control can connect vehicles and get the ability to drive close and as one unit. This can reduce drag and fuel consumption, and at the same time increase traffic throughput.

The advantage of using an image sensor for VLC for automotive use is that it can provide additional safety features, using image processing. Another step of security can be added with minimal additional cost.

Features like lane assist, pedestrian detection, verification of VLC to make sure received information corresponds to what the image sensor sees, collision warning and cruise control can be added for triple redundancy using DSRC, VLC and image processing.

ITS using VLC has a significant advantage that it can be used on existing infrastructure; only small modification is needed to give existing LED traffic lights and signs the ability to modulate its light to transmit data.

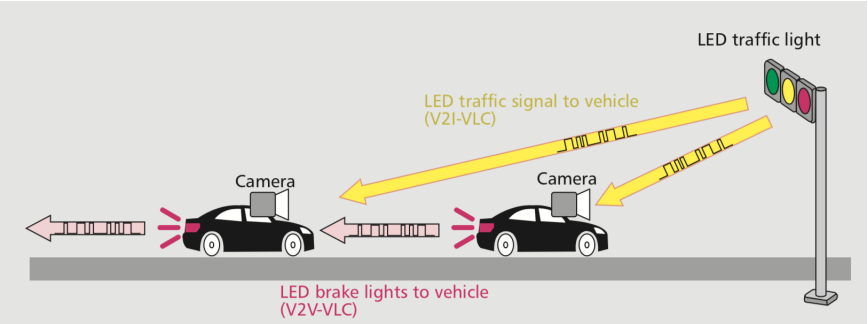

Figure 1.1: V2V VLC using headlights and brakelights. V2I using traffic lights and image sensor receiver [8].

1.3 Earlier work

There are a few different methods to receive VLC signals. One of the methods is using a single photodiode receiver. Single photodiode receiver has a big disadvantage that it cannot be used in situations with direct sunlight or other light pollution with high intensity because the sum of these signals will attenuate the actual signal to be received. The single photodiode receiver will not be able to discriminate between the different light sources, such as the sun, reflections, and other light sources, and will, therefore have a very low SNR. To combat these problems, the FOV of the photodiode can be decreased. A lower FOV will increase the SNR [1]. For automotive use, a low FOV single photodiode receiver cannot be used. This is because there will be a need for tracking of transmitting LEDs - to keep the transmitting LEDs inside of the FOV and image processing to find LEDs to track. Single photodiode VLC receiver for automotive use has been realized by, I.E. Lee et al. [9]. Their receiver differs from the traditional receiver in that it has better performance in daylight than conventional single photodiode receivers.

Another method of receiving VLC signals are image sensors that use a conventional integrating image sensor. This method captures a frame and then for each frame the transmitting LED is checked if it is off or on, assuming on-off keying modulation is used. The conventional image sensor has the disadvantage of being limited by framerate, readout speeds, and memory write speeds. High framerate image sensors are required for this type of VLC. Previous use of VLC uses an array of LEDs to transmit

data. This was done by using different encodings to modulate the LEDs in the array to have multi-bit transmission [8][10]. The transmission rate for this is limited by the framerate, which has to satisfy the Nyquist frequency requirement. A 1000 frames per second (FPS) image sensor could give data rate up to 500bps, however using a LED array as a transmitter, the data rate can be increased. This scheme of VLC is used for data transmission of a few kilobits amounts of data. The LED array used for transmitting data needs to have sufficient distance between the LEDs so that the LEDs are not perceived as one. Additionally, the distance between the LED array needs to be close enough that the receiver can detect separate LEDs.

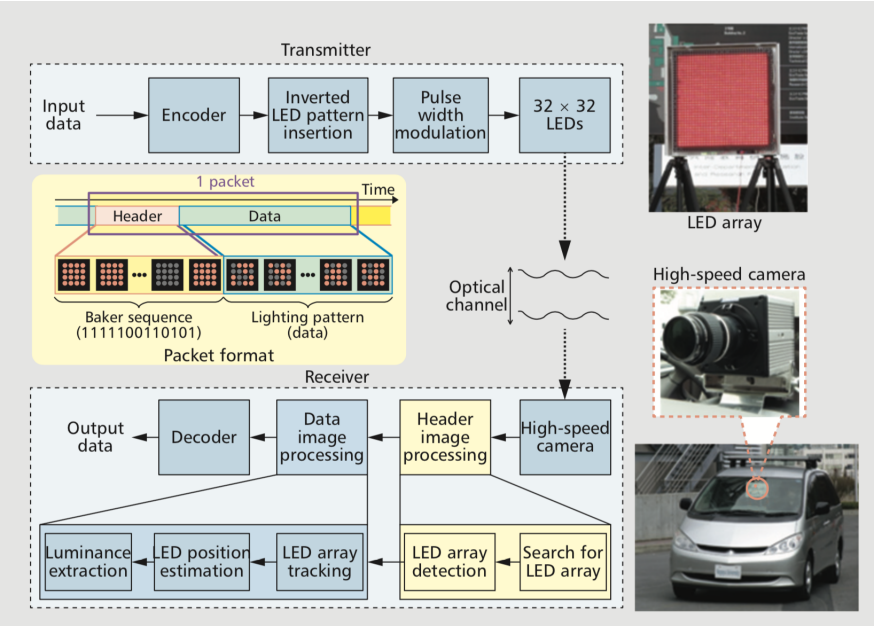

Figure 1.2: LED array transmitter used for V2I-VLC. This figure shows how data is processed and transmitted using LED array and high framerate camera. [8].

1.4 Photodiode

A photodiode is a device that converts a signal from the optical domain to the electrical domain. In this process, electromagnetic radiation is converted into electrical current in a device called photodiode. Electromagnetic radiation can generate electron-hole pairs in a semiconductor material when absorbed. An electron-hole pair is created when an electron is moved from the valence band into the conduction band. This free electron contributes to the conductivity of the semiconductor. To generate an electron-hole pair, the energy level of an electron needs to rise to equal or larger than the energy difference between the valence band and conduction band. This energy difference is called the band gap energy E_g. The band gap energy can be provided by an electromagnetic wave with photon energy which is at least high as the band gap energy [11]. The formula below

illustrates this relation

$$E_{photon} > E_g$$
$$\frac{h \cdot c}{\lambda} > E_g$$

Where h is Planck's constant, c is the speed of light, λ is the wavelength of the electromagnetic radiation, E_g is the bandgap energy of the semiconductor. According to the formula, the incident photons needs to possess the minimum energy equal to the band gap energy to create an electron-hole pair. Excess energy is dissipated as heat. The band gap energy of silicon is 1.12eV [12]. Using the formula above gives a wavelength of 1.11μm, which is very close to the infrared spectrum. Wavelengths below this posses the energy required to generate electron-hole pair in silicon at room temperature.

Electromagnetic waves that penetrate a semiconducting material gets gradually absorbed. Photons have an absorption coefficient that determines the depth in the semiconducting material the photons generate an electron-hole pair. The absorption coefficient is a constant which depends on the wavelength. Electromagnetic waves with longer wavelengths get absorbed deeper in the semiconductor material, while shorter wavelength gets absorbed close to the surface. Photons with wavelength above 1.11μm have a very low absorption coefficient and result in very long penetration depth. This is due to the lower photon energy, which is insufficient to create an electron-hole pair. These photons will travel through the semiconductor material without being significantly absorbed [11].

An electron-hole pair is created when an electromagnetic wave with sufficient energy hits either the n-type region, p-type region or the depletion region. The electric field of the depletion region separates electrons and holes, and they are swept to the region where they are majority carrier. The electron-hole pair created in the n-type and p-type region are recombined and does not contribute to the photocurrent. In CMOS process the depletion region is formed between the n-type material close to the surface as shown in Figure 1.4. This causes the depletion region to be close to the surface of the semiconductor material. Electromagnetic waves with longer wavelength get absorbed deeper into the substrate, and many of the generated electron-hole pair recombines and does not contribute to the photocurrent.

Three parts define the photocurrent of a photodiode; drift current, hole diffusion current which originates from the n-well and electron diffusion current. The electron diffusion current is generated in the substrate and is the most dominant contributor of photocurrent for longer wavelengths, while the drift current inside n+/p+/n-well regions and hole diffusion dominate for shorter wavelengths [11]. When the semiconductor material is exposed to a shorter wavelength of blue light, the electron diffusion current bandwidth is significantly increased compared to the longer wavelength of red light. This is because the electron diffusion current in the substrate is significantly slower than the hole diffusion current and

drift current. The slow electron diffusion originating from the substrate determines the response of photodiode exposed to long wavelengths and limits the conversion speed in the lower MHz range [11].

In a standard n-well CMOS process there are three ways to create a pn-junction as shown in Figure 1.3. The first one on the left is an n-well/p-sub diode. This diode uses the n-well to create the pn-junction in the p-substrate. The middle one is an n+/p-sub diode. This diode uses a smaller highly doped n-region to create a pn-junction. The highly doped n+ implant makes the depletion region smaller compared to the n-well/p-sub diode. In addition, the smaller depth of the n-region causes the diode to have less collection efficiency for longer wavelengths. The third diode is a p+/n-well/p-sub diode. This diode has an additional p+ layer on top of the n-well to create an additional pn-junction. These two pn-junctions creates a depletion region that is larger than the n-well/p-sub depletion region. The high hole concentration of the p+ layer makes this diode have a lower dark current compared to the n-well/p-sub diode. However, the depletion capacitance adds in parallel [13]. The maximum charge

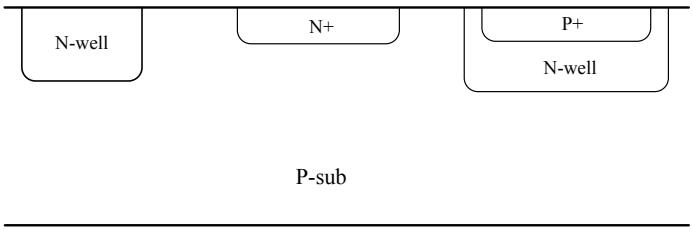

Figure 1.3: Three diodes for CMOS

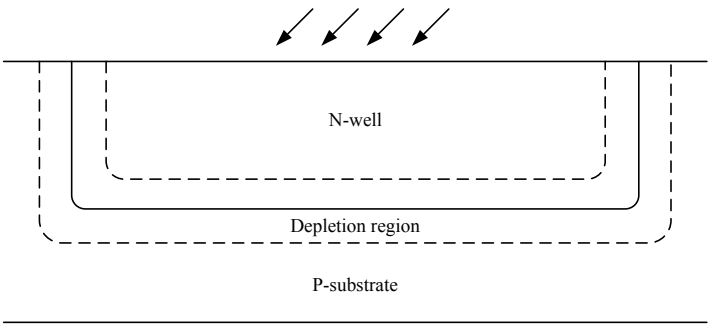

Figure 1.4: Cross section of nwell/psub diode with depletion region highlighted.

a photodiode can hold is called full-well capacity (FWC) and is usually measured in a number of electrons. When a photodiode reaches this limit, it is saturated, and an additional charge will be spilled over to neighboring photodiode well. This phenomenon is called blooming and can be seen as a bright spot glowing. This can be prevented by adding an overflow drain, mechanical shutter, and preventing the pixel from going into saturation with an electronic shutter. Another artifact created by strong light is called smear. Smear appears as vertical stripes that originates from a bright

spot. In CMOS process smear occurs rarely and is usually not a common problem. The FWC is a part in determining the dynamic range of an image sensor. The efficiency of a photodiode depends on different properties. Quantum efficiency (QE) is a ratio of incident photons to generated charge. For example QE of 0.4, this means that for every 100 incident photons, 40 photons are converted to a charge. The QE is affected by reflection from the surfaces such as microlens and silicon oxide. Some electron-hole pairs recombine fast and do not contribute charge. QE is also dependent on the energy of the photons.

1.5 Pixel

An image sensor consists of an array of pixels. Each pixel can have a different number of transistors combined with a photodiode. The three transistor (3T) is one standard configuration. The 3T pixel is configured so that one transistor works as a reset for the photodiode; one works as a source follower and one as a select switch between the source follower and the output column which are connected to all pixels in a column. A pixel with signal amplification capability is called an active pixel. The source follower in the pixel provides the signal amplification. In the 3T pixel architecture, the photodiode is connected to the floating diffusion (FD) node. In 3T pixels, the FD node is the node where the output of the photodiode is connected to both the reset transistor and the gate of the source follower as shown in Figure 1.5. This node is where the charge generated by the photodiode is stored. The operation of the 3T pixel works as: First, the photodiode is reset to VDD by the reset transistor. Then the photodiode discharges the FD node for a given integration period. The source follower buffers the voltage on the FD node and is read out when the pixel is selected.

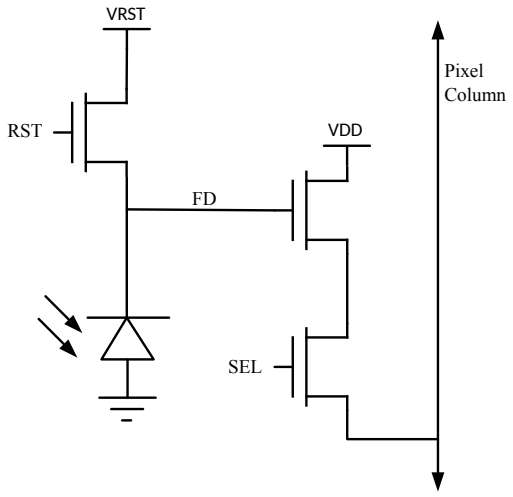

Figure 1.5: Configuration of a 3T active pixel.

Another pixel configuration is the 4T pixel. The 4T pixel uses a

photodiode with a p-type pinning layer on top of the n-well. The pinned photodiode realizes no image lag, low noise, low dark current, high sensitivity, and electric shuttering [14]. This pixel has an additional transistor between a pinned photodiode and the reset transistor as shown in Figure 1.6. This advantage makes the 4T pixel a good alternative to the 3T pixel. Additional transistors can be added to the pixel to create a desired pixel operation. Connecting the gate of the reset transistor to its

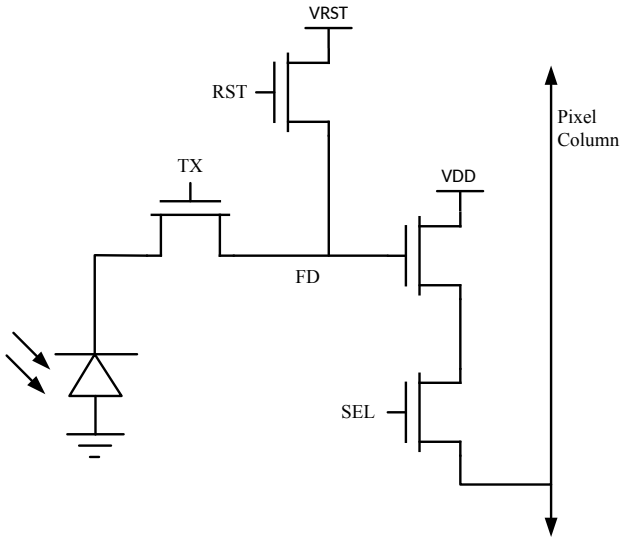

Figure 1.6: Configuration of a 4T active pixel.

drain, the transistor turns into a diode connected transistor operating in the subthreshold region. This diode-connected transistor is used to create an output voltage that is logarithmic to the photocurrent from the photodiode. The advantage of logarithmic operation is the increased dynamic range to six decades or 120dB, compared to the standard active pixel which has a dynamic range of 60-70dB [15] [16]. A logarithmic pixel has the advantage

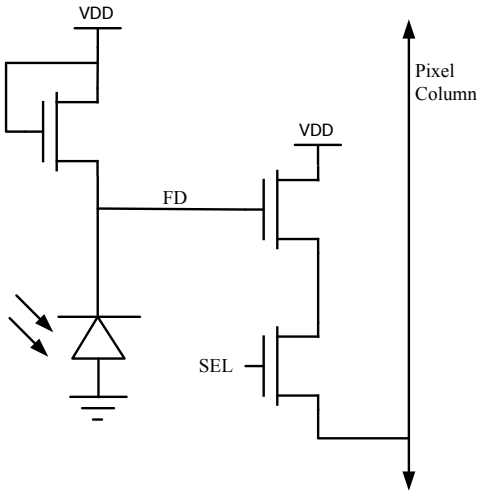

Figure 1.7: Configuration of a log pixel.

of a continuous output voltage and does not require an integrating period as the 3T or 4T pixel. Disadvantages of a logarithmic pixel are that it has a low output voltage swing of only around 0.2V to 0.3V [16]. However, it is also possible to add another diode-connected transistor between the diode-connected transistor and VDD to double the output voltage [17]. Using a logarithmic pixel has one major drawback compared to the active pixel, and that is fixed pattern noise (FPN). Logarithmic pixels are more sensitive to the difference in threshold voltages, which gives more FPN than active pixels [15] [16] [18]. Another disadvantage is that logarithmic pixels need calibration to capture images with good quality. However, to find a light source in the image, a low noise image is not required.

These advantages show that an image sensor for VLC profits from using logarithmic pixels to achieve sufficient throughput. One sensor that uses logarithmic pixels and 4T pixels, and has 15Mbps output and real-time tracking of the light source have been developed [19]. This image sensor consists of a pixel array with alternating pixel topologies, one for image and one for communication. The imaging pixels are 4T which are used to create a 1-bit flag image to get the spatial position of a light source. Spatial coordinates found by the image pixels are then used to find the pixel to be used for receiving. The communication pixel is a logarithmic pixel, which has been designed for optical signal reception. In their communication pixel, they used a component equivalent to an n-channel junction gate field-effect transistor (n-ch JFET) biased by GND. They have also reduced the FD node capacitance, by using a depleted PD with floating diffusion (FD) and charge overflow drain. When they used a depleted PD with a pinned layer, the sensitivity and response speed were increased because of the reduced capacitance in the depleted region.

1.6 Image sensor

CMOS technology gives the possibility to implement more components into the image sensor chip. Noise reduction circuits, ADC, amplifiers, timing, signal processing, control circuits and more can be implemented on the same chip. Microlens array is small lenses placed on the surface of an image sensor. The purpose of the microlens array is to focus the light into the photosensitive part of the pixel, thus increasing the sensitivity. Information about the amount of red, green and blue (RGB) light present in the scene must be measured, to create color images. This is done using a color filter array (CFA). The CFA is a mosaic of alternating color filters that pass red or green or blue light. This gives the pixel information about the amount RBG light present. Each pixel captures information about a single color of RGB, to get a color image, interpolation is used to create an RBG value of each pixel.

1.7 Noise

Noise in image sensors is an unwanted signal that deteriorates the image quality. A noise that is fixed at a spatial position is called fixed pattern noise (FPN). The other noise is the time-dependent random noise referred to as temporal noise. The noise floor is the minimum level a pixel can have, and this level defines the lower end of the dynamic range.

1.7.1 Fixed pattern noise

Fixed pattern noise is noise in images that are usually perceived as vertical stripes. This noise is caused by dark current nonuniformity, photo-response nonuniformity and process variation in the column amplifier, threshold voltages, offset and gain. Each column has a column amplifier, a difference in threshold voltage causes an offset in every pixel that shares that column amplifier. FPN can be reduced or removed with black level subtraction (BLC). BLC works by first capturing an image in total darkness, then removing the values captured to the image taken which should give an image. Black level is the reference black for the image sensor. Optical black (OB) pixels are used to capture the temperature dependent dark current in the image sensor. OB pixels are usually placed around the pixel array and are covered to prevent light from getting into the photodiode. The captured dark current from OB pixels is subtracted to the image in the signal processing step. Logarithmic pixels are more sensitive to process variation compared to integrating pixels with a reset operation [18]. One reason is that logarithmic pixels do not have the noise removing circuitry available because it does not have integration operation. Figure 2.11 shows an image captured on a logarithmic image sensor.

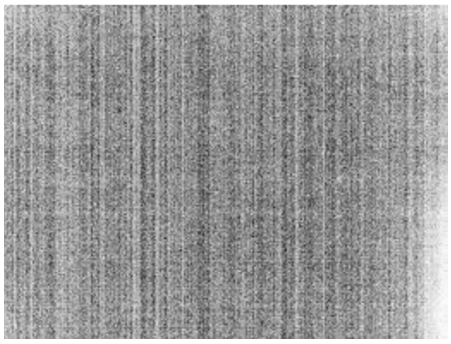

Figure 1.8: Fixed pattern noise [20].

1.7.2 Temporal noise

Temporal noise can be caused by photon shot noise, dark current shot noise, thermal noise, reset noise, pixel source-follower noise. This type of noise is random and will be different each time an image is captured. The random temporal noise is not as visible as FPN, and more effort is put

into suppressing FPN. Figure 1.9 shows what effect temporal noise has on image quality.

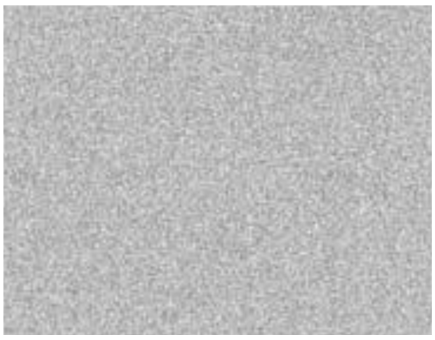

Figure 1.9: Temporal noise [20].

1.8 Noise suppresion

The conventional active pixel image sensor has a significant advantage in noise reduction possibilities over logarithmic pixels. Active pixel image sensors can implement a noise reduction scheme that removes reset noise. This scheme is called correlated double sampling (CDS). CDS works by sampling the pixel value at a known state in the reset period, then sampling again after at the end of the integration period. Subtracting these two values will give a signal value that has no reset offset, reduced flicker noise, and FPN [21] [22]. However, a pinned photodiode is required to achieve complete removal of reset noise and reduced read noise. Another noise reduction scheme is differential delta sampling (DDS). DDS circuit is used to remove offsets due to the column drivers, and hence reduces column-to-column fixed pattern noise [22]. However, these noise suppressing techniques are not available for logarithmic pixels.

1.9 Dynamic range

Dynamic range is defined as the ratio between the full-well capacity and the noise floor, which corresponds to highest to lowest luminance. This ratio is usually expressed in a logarithmic scale, typically in decibels. Full-well capacity is the maximum amount of charge that can be accumulated on a photodiode capacitance, and the noise floor is the noise that comes from the readout electronics and the amplifier inside the pixel [21]. The wide dynamic range of our vision makes it possible to see what is on the outside at the end of a tunnel, where the traditional image sensor will be saturated and will show a white wall. For automotive use, a high dynamic range operation is necessary.

1.10 Decoder

To address each pixel for readout, decoders are necessary. Every pixel has an X and Y address and can be accessed with the use of decoders. A row decoder is needed to select a row to be read. A column decoder is needed to select a column to access the pixel at the selected row and column address. The readout sequence works by first selecting a row, then the column decoder selects every column sequentially, and this scheme requires the column decoder to have a faster operation than the row decoder.

There are two types of decoders used for pixel addressing. The first one is a shift register. Shift register scanner works by sequentially iterating through all columns. The advantage is a simple configuration, and lower noise generation as less switching happens. The drawback is that it is less flexible than an addressable decoder, as it can not be addressed to select a single pixel. The other type is the addressable decoder. This decoder is very flexible and can select a single pixel or an area of pixels to read out. However, it requires more area and more switching that can cause noise. Worst case scenario for a binary decoder is when n-1 bits changes, and can cause glitching and increased noise. A way to combat this is to use a grey code decoder. Grey code is a binary number system where an increment of value changes only a single bit. Using a gray code decoder has the advantage of making it less prone to cause glitching and noise.

Rolling shutter is the most common capturing scheme used for CMOS image sensors. The advantage of rolling shutter is that there is no need for an extra transistor for buffering in each pixel. When the pixel is read, the value is transferred straight to the readout circuitry which could be CDS circuit at the bottom of the column. The disadvantage of rolling shutter scheme is fast moving objects will be skewed because the rows at the bottom of the image sensor are readout later than the rows at the top. An example is propeller blades which will look bent as shown in Figure 1.10. The rolling shutter scheme for pixels with reset operation

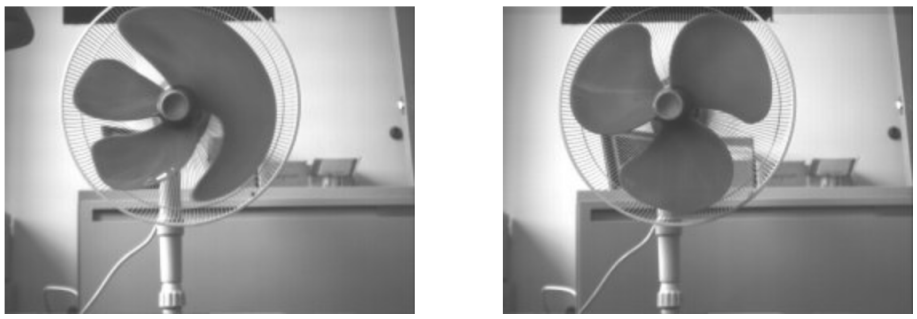

Figure 1.10: Image illustrating the effect of capturing a fast moving object with a rolling shutter scheme. Rolling shutter is used to capture the image on the left, and global shutter is used to capture the image on the right [23].

requires a row decoder with both row address output and reset output. The sequence consists of first resetting the photodiode by removing the charge accumulated. Then the select transistor outputs the photodiode value. The

time between the pixel is reset, and the pixel is selected, is the exposure time.

Global shutter scheme is an alternative to the rolling shutter scheme. Global shutter works by resetting every pixel at the same time, then the capture the scene by moving every pixel value to a buffer. The buffers are then sequentially read out. This scheme is desirable over rolling shutter because the entire frame is captured at the same time, preventing the distortion of the rolling shutter scheme. The disadvantage of a global shutter is the requirements of either an in-pixel memory or a frame memory. This requires more chip area, and commonly seen only in high-end image sensors. A global shutter can be used in 4T active pixels. However, it is not recommended for practical use [24].

Part II

Design

Chapter 2

Design

2.1 Top level

The image sensor consists of five main components. The first component is the pixel array which consists of 128x128 pixels. Addressing these pixels can be done with a row and a column decoder. To get the voltages out of the pixel array a current source is needed, and to drive the large pad of the pad frame a large buffer is needed. Top-level diagram is shown in Figure 2.1. The relations between the different components are shown in this figure. The row decoder has 128 addressable outputs which are used for selecting

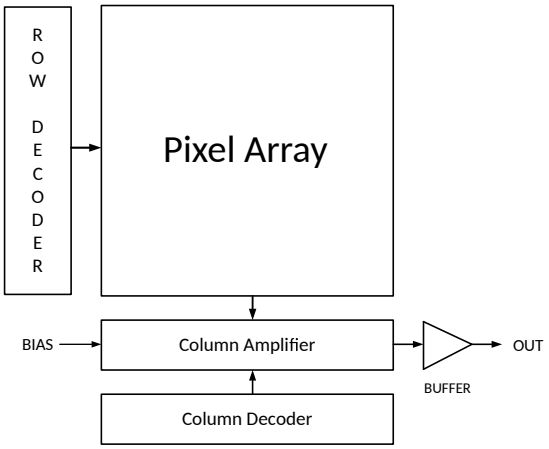

Figure 2.1: Top level schematic of the image sensor.

the row for readout. The pixel array has 128 column lines which are connected to the column amplifier block at the bottom. This block contains the current sources needed to read out voltage from the pixels. This block also contains the column select transistor. A horizontal wire running across the column amplifier block provides bias voltage for the current sources. The column decoder is placed below the column amplifer block and has 128 column select outputs for the column amplifier block.

2.2 Photodiode

The photodiode was first selected to be PHDNWA850, a photodiode provided by the AMSC35OPTO process. During the final stages before tapeout, the process was changed from AMSC35OPTO to AMSC35B4. One of the layers of photodiode PHDNWA850 is unique for the OPTO process and made the photodiode unavailable for the new process. The layer that was made unavailable was a definition layer in PHDNWA850, and the problem was solved by creating an identical photodiode in the new process without the unavailable layer. Creating an identical photodiode with the same dimensions made it possible to swap PHDNWA850 with the new photodiode. A cross section of the photodiode is shown in Figure 2.2, this figure shows the layers that builds up the photodiode. The minimum width and length of PHDNWA850 are $5\mu m$. The width and length parameter is defined for the photosensitive area. Additionally, PHDNWA850 has a guard ring surrounding the photosensitive area, which increases the photodiode width and length to 7um.

The photodiode consists of a photosensitive part in the middle and is where the photoconversion happens. Contacts for the well is located at the bottom of the photosensitive area as shown in Figure 3.1, this is where the photodiode is connected to the drain of the diode-connected transistor, and the source follower gate. A simulation model for PHDNWA850 was

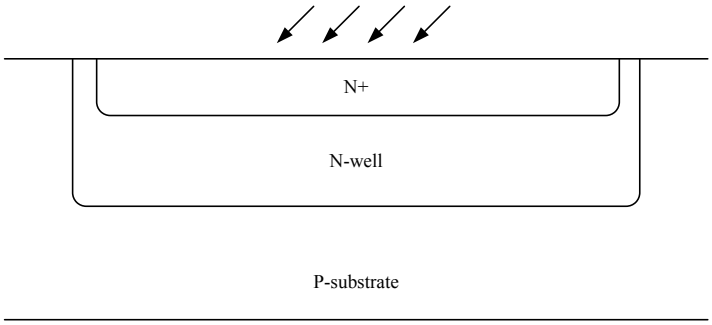

Figure 2.2: Cross section of PHDNWA850. Guard ring not shown in Figure.

provided. The symbol for the simulation model has three pins, where two of them are for the diode, and an input pin which controls the photocurrent gain. This port is a voltage controlled current source that models the photocurrent generated by the diode. Increasing the input voltage increases the output current. This relation is shown in Figure 2.3, this figure shows that the input voltage and the output current is constant. However, the photodiode that was used is not PHDNWA850; we can assume the operation and outputs to behave similarly.

The cut-off frequency is dependent on the amount of photocurrent the photodiode outputs, and the components that determine the cut-off frequency was explained in chapter 1.4. Figure 2.3 shows the relation between the input voltage and the output current. The input voltage is 2.941 times larger than the output current.

Different transient analysis of the FD node is shown in Figure 2.4,

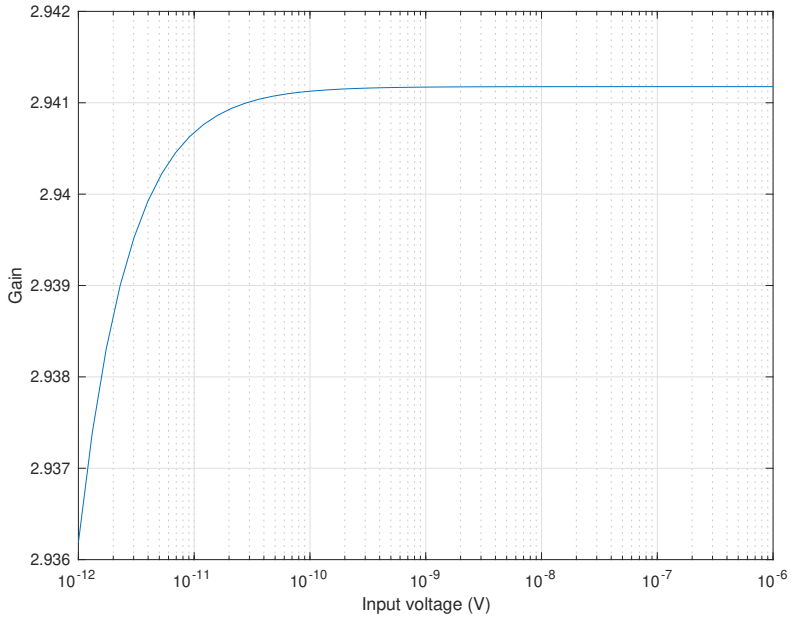

Figure 2.3: This plot shows the difference between the input voltage and output current of the simulation model for PHDNWA850.

Figure 2.5, Figure 2.6 and Figure 2.7. These figures show how the voltage on the FD node corresponds to different output currents from the photodiode. The output current swing in these figures are also very large and corresponds to large changes in luminosity. These large swings are only likely in the dark when a light source with high optical power output transmits modulated light. However, in daylight, the difference between on and off is not as significant as most of these figures illustrates. These figures show that the higher the output current is, the higher the bandwidth is achievable. Even when the output current swings between one decade. Figure 2.8 shows a more realistic plot, where the output current swings between 800pA and 400pA. With this output current swing, the FD node voltage swing is around 20mV. Simulations show that the output voltage from the chip is half of what the voltage on the FD node is. This reduces the output voltage swing to 10mV in this case. A 10mV voltage swing is small, and the signal to noise ratio might be too small. In Figure 2.4 the PHDNWA850 input is a square wave at 1MHz that swings between 30nV and 1nV, which gives an output current swing between 10nA and 1nA. The peak to peak voltage in the FD node is measured to be around 115mV as shown in Figure 2.4, and the output voltage of around 60mV. The rise and fall time is dependent on the amount of current the photodiode outputs. These figures also show that the fall time is faster than the rise time, fall time is when the light is in on position, and the rise time is equal to the off position which is when the light is off. The DC sweep of the input of PHDNWA850 is shown in Figure 2.9. This figure shows the total voltage range of PHDNWA850. In Figure 2.7 the output current from

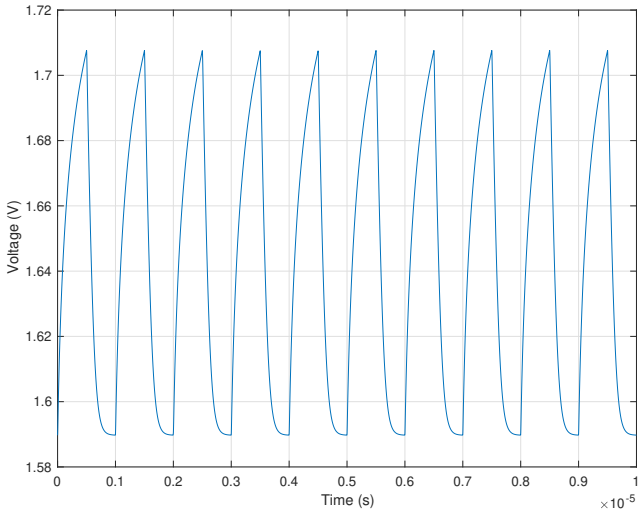

Figure 2.4: This figure shows the FD node when the input to the photodiode is a square wave with a frequency of 1MHz, the photodiode output current swing between 1nA and 10nA.

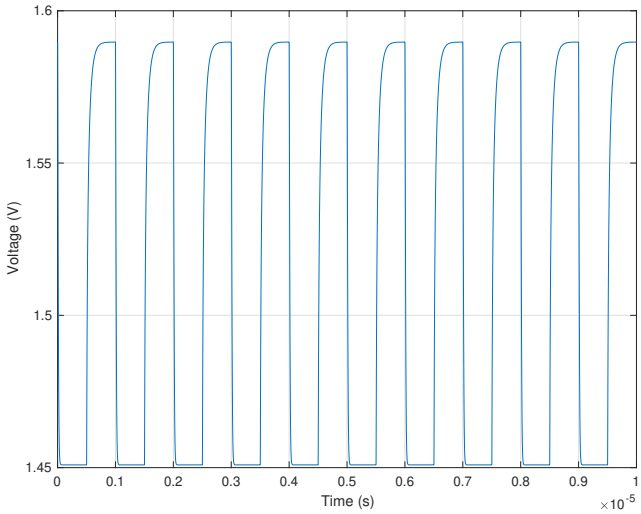

Figure 2.5: This figure shows the FD node when the input to the photodiode is a square wave with a frequency of 1MHz, the photodiode output current swing between 10nA and 100nA.

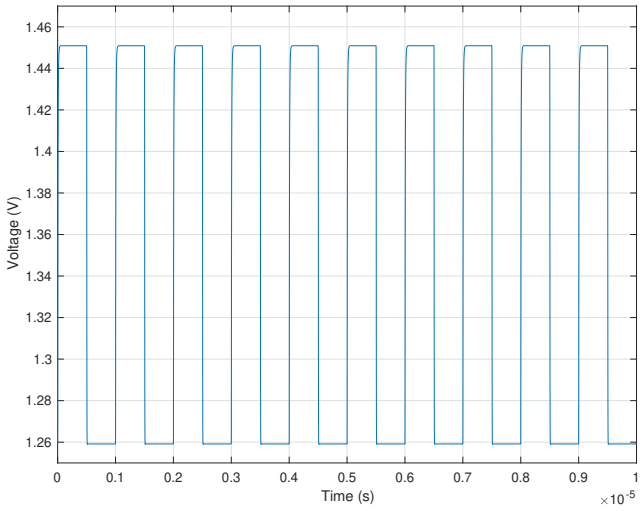

Figure 2.6: This figure shows the FD node when the input to the photodiode is a square wave with a frequency of 1MHz, the photodiode output current swing between 100nA and 1uA.

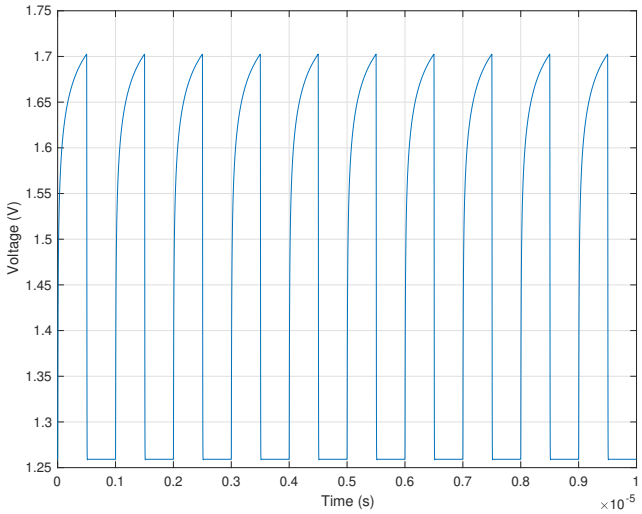

Figure 2.7: This figure shows the FD node when the input to the photodiode is a square wave with a frequency of 1MHz, the photodiode output current swing between 1nA and 1uA.

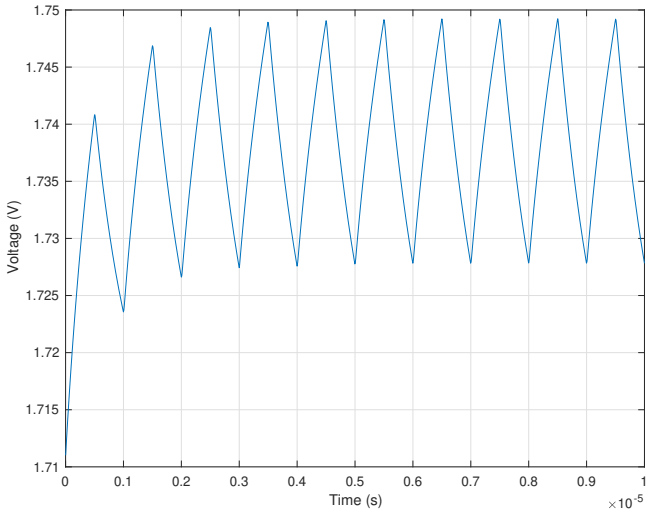

Figure 2.8: This figure shows the FD node when the input tot he photodiode is a square wave with a frequency of 1MHz, the photodiode output current swing between 400pA and 800pA.

the PHDNWA850 swings three decades from 1nA to 1uA, which equals to 438mV voltage swing. Since the input voltage is constant to the output current, the x-axis of Figure 2.9 could be substituted to output current and still get the same curve. A comparison between single and double diode-connected transistors is shown in Figure 2.13. The figure shows the increased voltage range and increased voltage per decade.

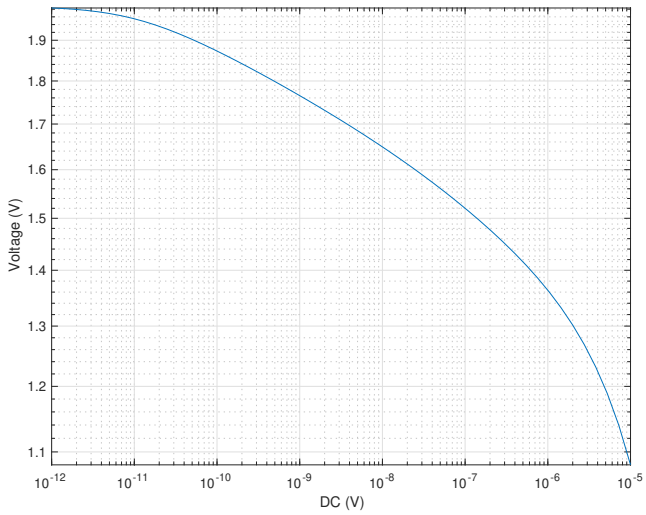

Figure 2.9: This figure shows the FD node when the input pin of PHDNWA850 is swept from 1pV to 10uV. The large dynamic range can be observed by the 6 decade range between 1pV to 1uV.

2.3 Pixel

In this project, a single pixel topology solution for both image readout and single pixel high bandwidth readout is explored. The pixel needs to do two different types of operation. First, it needs to be able to capture an image that has sufficient image quality so that a light source can be identified, and extract its spatial coordinates as shown in Figure 2.10. Second, after it has identified the light source used to transmit, it should be able to receive modulated light signals at a sufficient speed, which is at least in the megabits per second range. A logarithmic pixel was chosen because of its advantages that it can operate continuously, without a reset period. This ability makes it possible to achieve higher reception speed compared to an integrating pixel. The disadvantage of using a logarithmic pixel is that it is more sensitive to differences in the process and mismatch, causing a significant noise in the image captured. This is one reason logarithmic pixel is not used in conventional consumer still imaging cameras. However, in this case, large amounts of noise is not a problem as long as light sources can be detected in the image. An image captured with a logarithmic pixel image sensor is shown in Figure 2.11. This image illustrates the amount of noise an uncalibrated logarithmic image sensor contains.

The pixel consists of four transistors as shown in Figure 2.12. One which operates as a source follower, one which operates as a row select, and two which are diode-connected, with its gate to source. These two diode-connected transistors are the ones that differ from a traditional integrating pixel. Instead of reset connected to the gate of the reset transistor as shown in Figure 1.5, it is connected to drain. Two transistors are used in this configuration to double the logarithmic compression and almost double

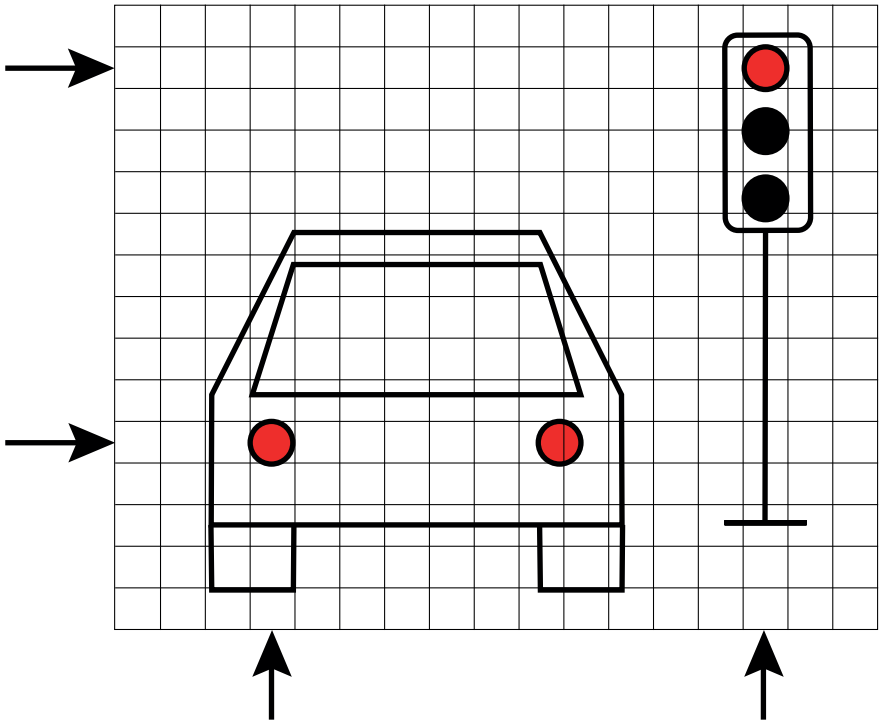

Figure 2.10: The grid illustrates pixels. The arrows illustrates which column and row has a light source for optical communication.

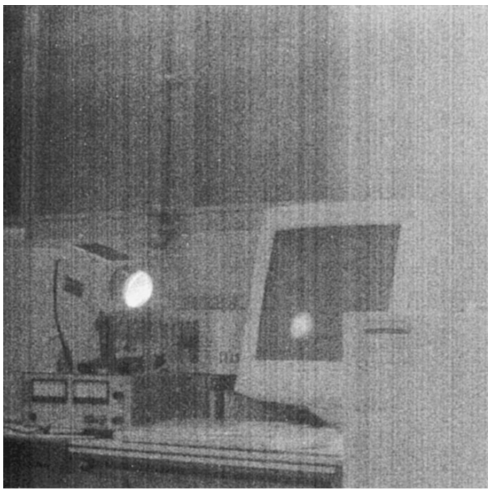

Figure 2.11: Image captured by an 512x512 logarithmic image sensor [18].

the output voltage swing. Doubling the voltage swing of the pixel gives the image sensor more room to differentiate between when the light received is logic high or low.

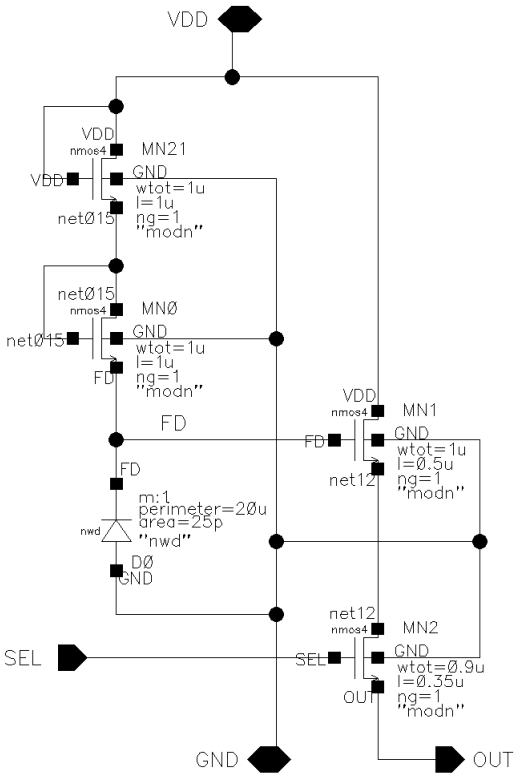

Figure 2.12: Schematic of the pixel used.

Comparison between single and double diode-connected transistors shown in Figure 2.13. This figure shows the advantage of adding a diode-connected transistor. Adding a third diode connected transistor increases the mV/dec. However, the threshold voltages of the diode-connected transistor decrease the output voltage to a level that is undesirable. The photodiode will convert this light into current and reduce the voltage of the FD node. The speed of this operation is limited to the bandwidth of the photodiode and readout path.

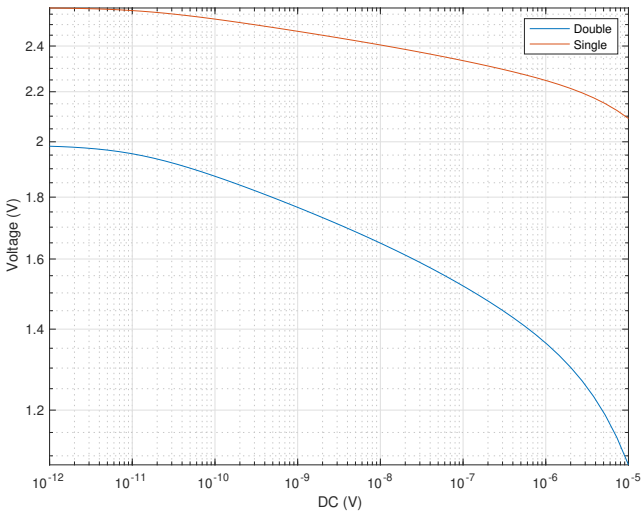

Figure 2.13: This figure shows a comparison between the single diode-connected transistor shown in Figure 1.7, and double diode connected transistor used in this project shown in Figure 2.12.

2.4 Column amplifier

The current source is located at the bottom of every pixel column in the column amplifier block. Schematic of the column amplifier component is shown in Figure 2.14. P_OUT is where the pixel column is connected with a current source and PMOS source follower. The source follower is then connected to the column select transistor. The large width of the transistors is chosen to be less susceptible to process variation and mismatch.

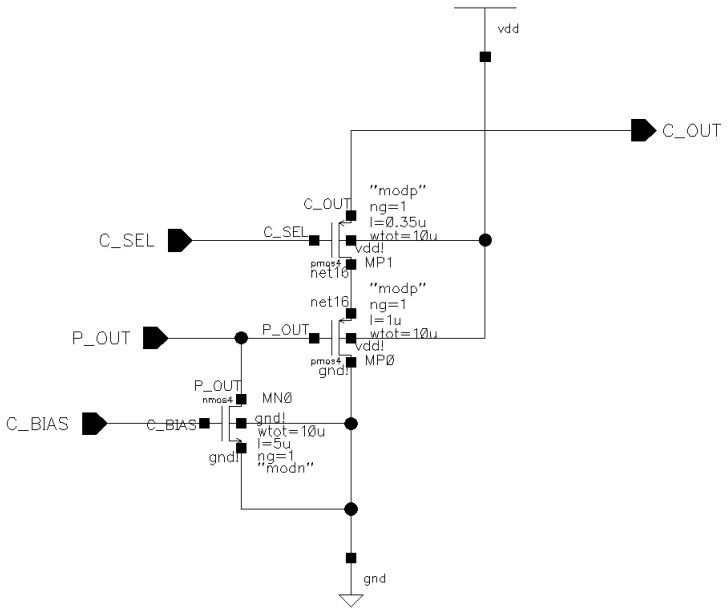

Figure 2.14: Schematic of the current source at the bottom of every pixel column.

2.5 Decoders

The decoders used, are the same as the column decoder used by Soman Cheng and Marius Lillestøl [25], which was based on the decoder design of Mathias Wilhelmsen and Stian Hjortset [26]. The decoder has a gray-code input, which has the advantage of only switching one bit to increment address. This reduces the chance of glitching and power consumption. The column decoder is active low, because of the pMOS column select transistor. The row decoder is identical to the column decoder, except one added component on the outputs. By adding an inverter to the outputs of the column decoder, an active low decoder suitable for addressing nMOS select transistors in the pixels is made.

The conventional row decoder for an integrating pixel image sensor consists of 2^n addressable outputs and reset outputs. The row decoder for this image sensor is simpler than the conventional row decoder because there is no need for reset output. A column decoder is a component that selects the column to be read. For a conventional integrating image sensor, this component can as simple as a shift register that iterates through the columns. In this project, decoders have two different operations, and an addressable row decoder and a column decoder is needed. The first type of operation is capturing an image. In this operation, the decoders use a rolling shutter scheme. For every row, the column decoder iterates through every column. The other type of operation is receiving mode, where the decoders get the spatial address for a pixel to be used for reception.

The decoder is built up using alternating layers of NAND and NOR

logic arranged in a symmetrical binary tree. To get the gray code operation every other decoder is mirrored as shown in Figure 2.15, Figure 2.16, Figure 2.17, Figure 2.18. These smaller 1-2 decoders are connected together to create a 4-16 decoder as shown in Figure 2.20. Which are used to create a 7-128 decoder as shown in Figure 2.21.

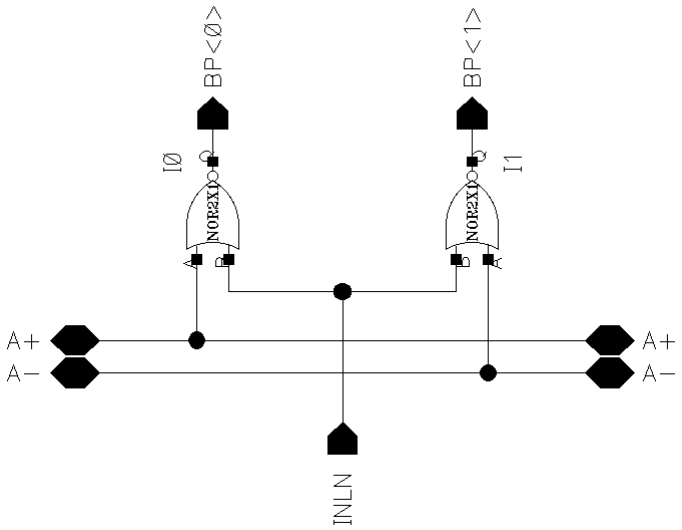

Figure 2.15: Schematic of 1-2 decoder. The input is active low and the output is active high.

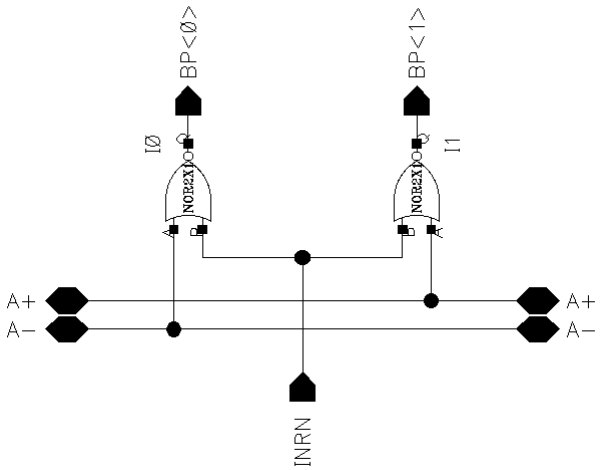

Figure 2.16: Schematic of Figure 2.15 mirrored.

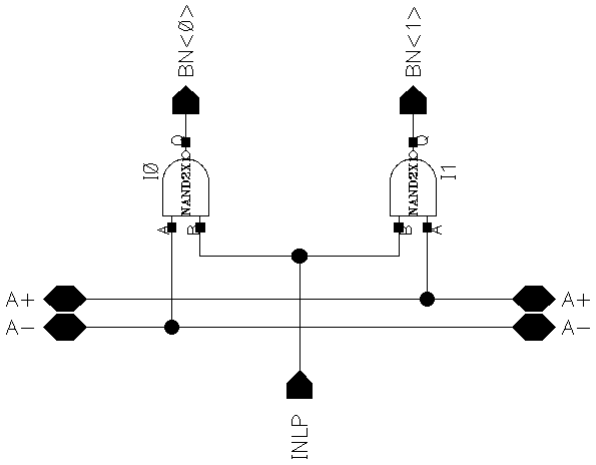

Figure 2.17: Schematic of 1-2 decoder. The input is active high and the output is active low.

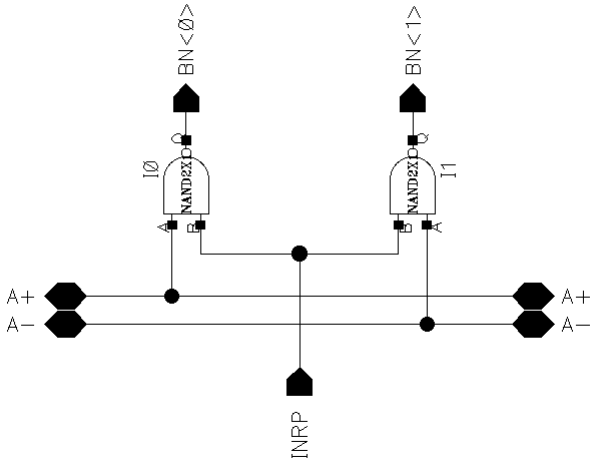

Figure 2.18: Schematic of Figure 2.17 mirrored.

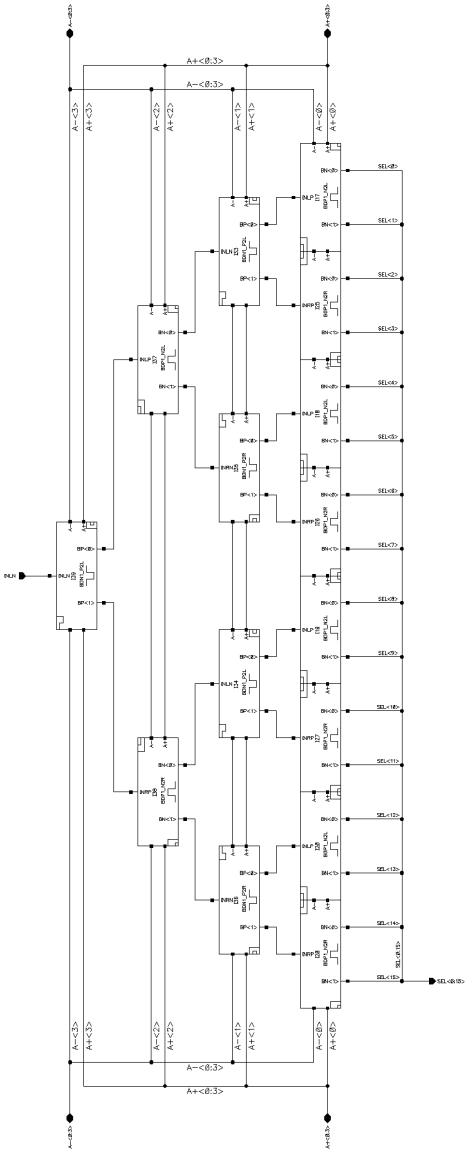

Figure 2.19: Schematic of one of the 4-16 decoder. This decoder is built up 1-2 decoders shown in Figure 2.17 and Figure 2.18 and Figure 2.15 and Figure 2.16

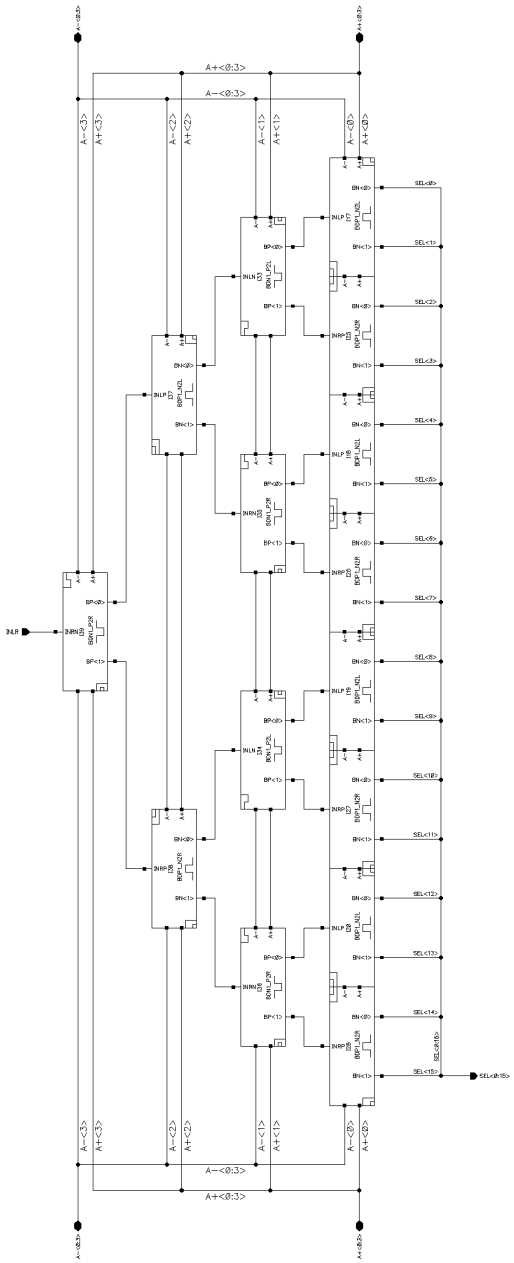

Figure 2.20: Schematic of the other 4-16 decoder. This decoder is built up 1-2 decodeers shown in Figure 2.17 and Figure 2.18 and Figure 2.15 and Figure 2.16

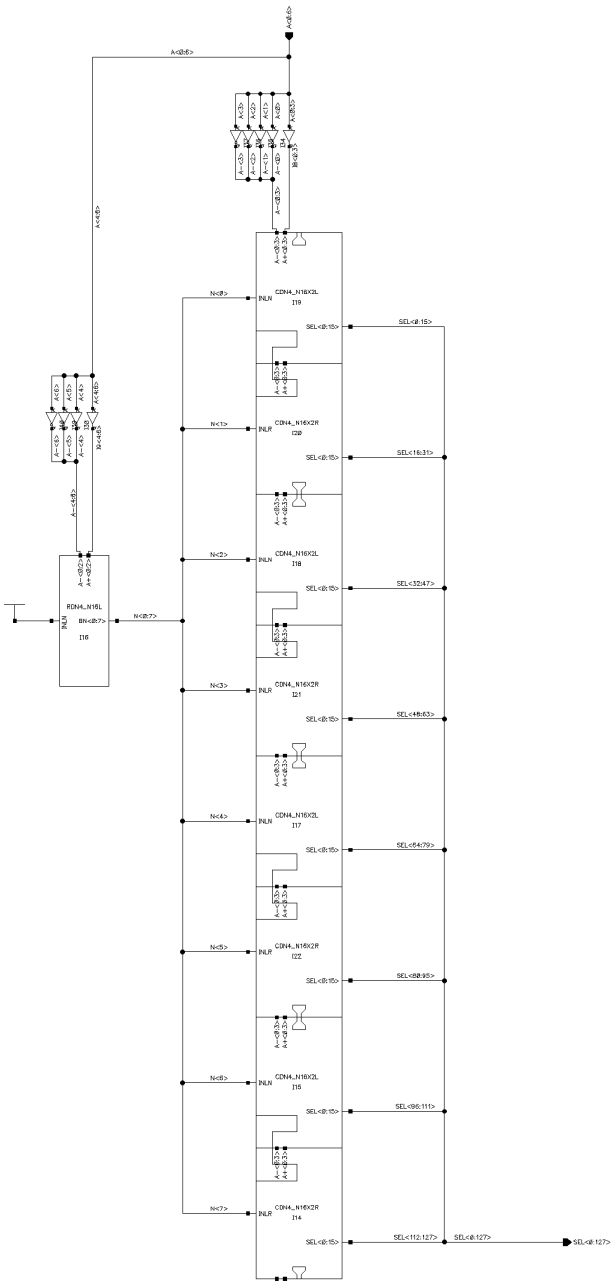

Figure 2.21: Schematic of the 7-128 column decoder. This decoder is built up by the 4-16 decoders shown in Figure 2.19 and Figure 2.20 in an alternating configuration.

2.6 Output buffer

An output buffer was provided by Philipp Hafliger. The purpose of the output buffer is to buffer the signal and drive the pad and its capacitive load. AC analysis of the buffer is shown in Figure 2.23. As seen in the figure the buffer cut-off frequency is 47MHz. For this application, it is sufficient because the bandwidth is limited to a few megahertz by the photodiode. AC analysis with 15pF load is also shown in the figure, and this shows the effect the large capacitance has on the bandwidth. In the AC analysis, the buffer was biased with 1V. The bandwidth of the buffer correlates to the bias voltage increasing bias voltage increases the bandwidth. In image capture mode high bandwidth is not needed, and the bias voltage can be decreased.

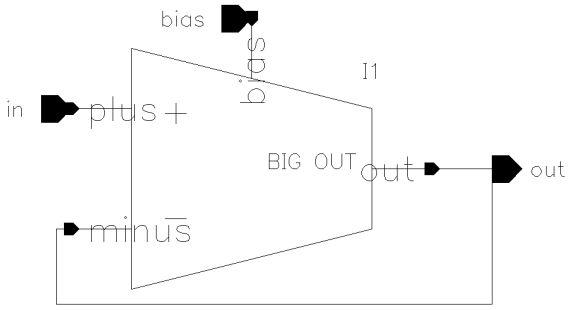

Figure 2.22: Symbol of the buffer.

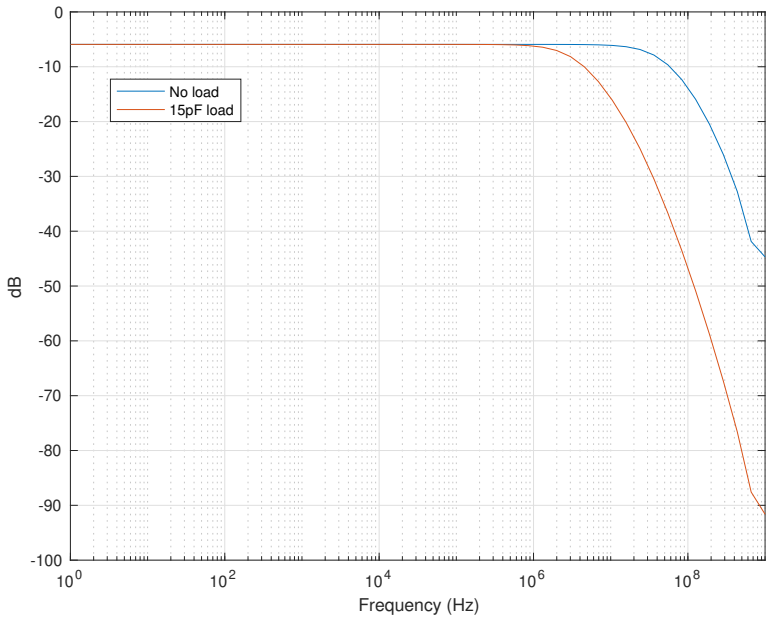

Figure 2.23: AC analysis of the buffer.

2.7 Readout

A simplified schematic of the readout path of the image sensor is shown in Figure 2.24. M1 and M2 are the diode-connected transistors which provide the pixel with a logarithmic operation. M3 is the source follower transistor connected to M4 which is the row select transistor. M5 is the current source at the bottom of the column line, where all row select transistors in the column are connected. M6 is the source follower which is connected to the column select M7, which connects to the horizontal output line that is connected to all the column selects. M8 is another current source for the output line. The output buffer mentioned in the last section is connected to the right end of the OUT line. PEX extraction shows that the capacitance

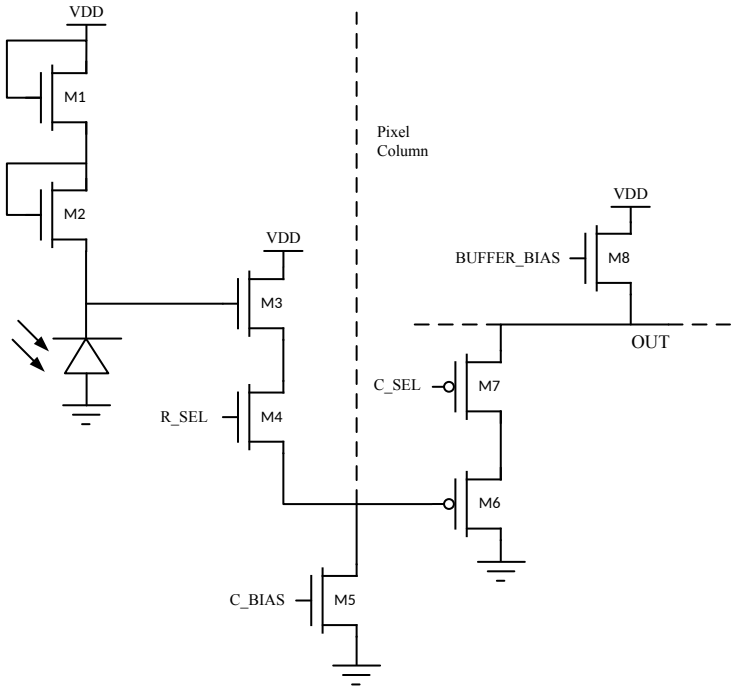

Figure 2.24: Schematic of pixel and readout path.

on the output node that connects column amplifiers to the output buffer has a capacitance of 0.58fF. The pixel column that connects 128 pixels into a column has a parasitic capacitance of 0.35pF. Using these values, the expected cut off frequency can be determined. AC analysis of the readout path is shown in Figure 2.25. The voltage for the analysis is applied to the input of the column amplifier. A bias voltage of 1V was used for the column current source and output line current source. A 15pF load was added on the output of the output buffer. The bandwidth was measured to be 6.1MHz.

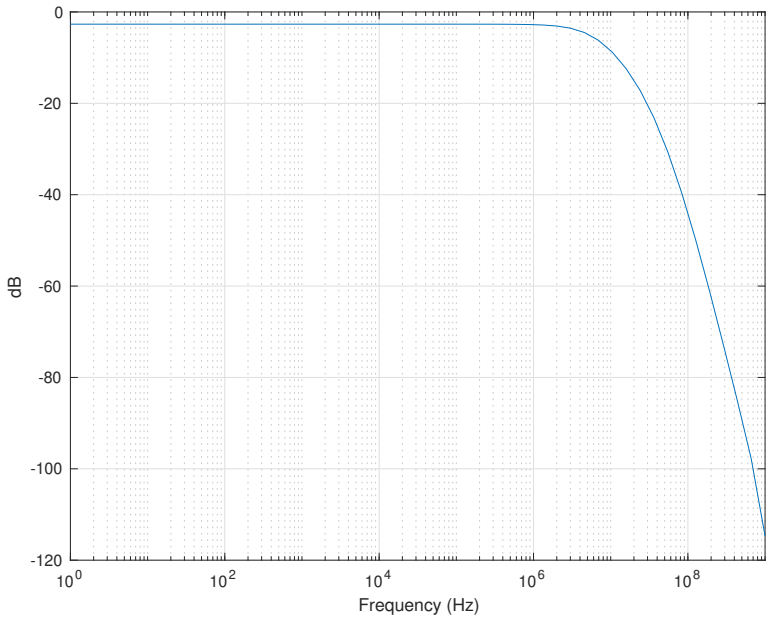

Figure 2.25: AC analysis of the readout path.

Chapter 3

Layout

3.1 Pixel

The pixel was designed to connect to the surrounding pixels when configured in an array. This means that all metal layers, horizontal and vertical wires are present in each pixel, and no additional wires need to be drawn when configured in an array. The pixel consists of four transistors, which are divided into two groups; one group where the diode-connected transistors share a well, the second group is the source follower and the select transistor, which also share a well. The photodiode is placed in the upper left corner of the pixel and occupies $7\mu m$x$7\mu m$ of area. This gives $2.25\mu m$ of space available on the right and bottom side of the photodiode. The guard ring around the photodiode is connected to ground. The fill factor of the pixel is 19.7%.

Pixel size is $11.25\mu m$x$11.25\mu m$ and was chosen to be $11.25\mu m$ to fit the column and row decoders which were designed with a $11.25\mu m$ pitch. The first pixel iteration was $1\mu m$ shorter both in height and width but was increased to the current size when the decision to use the column decoder from Soman Cheng and Marius Lillestøl [25] [27] was made. With the added space, the transistor sizes were increased as much as possible to reduce mismatch. The layout of the pixel is shown in Figure 3.1. Metal 4 (M4) is used for shielding and for VDD. The earlier pixel iterations had the M4 shield to the edge of the photosensitive part of the photodiode, but later the opening of the photodiode was increased. This was to reduce the chance of shadowing that occurred in Marius Lillestøl and Soman Cheng's pixels when the incident light was not perpendicular to the pixels [27]. Metal 2 is used for the pixel select. This line runs horizontally through the pixel and is connected to the gate of the select transistor. Metal 3 is used for the vertical output line. The vertical output line runs vertically through the pixel and connects the output of every pixel in the pixel column to the column amplifier module at the bottom. Metal 1 is used for ground. The guard ring around the photodiode is connected to two lines which run vertical on the left side and horizontal on the top of the pixel. This was added to create a grid of ground wire when the pixels are arranged in an array. The photodiode has the same dimensions as the AMS photodiode.

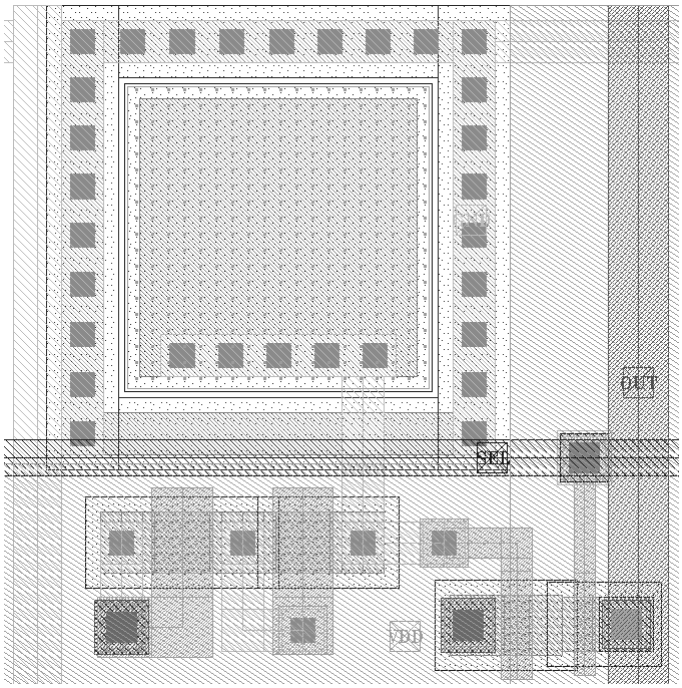

Figure 3.1: Layout of pixel used in this project. Schematic shown in Figure 2.12.

3.2 Pixel array

The pixel array consists of 128x128 pixels. The array is built up by pixels that are arranged by first creating a pixel column module which consists of 128 vertically stacked pixels. Then 128 of this module is horizontally stacked creating a 128x128 pixel array. The relation between pixels when they are placed side by side is illustrated in Figure 3.2, where four pixels are connected in an array configuration. The figure shows that there is space on the left and right side of the photodiodes. This space could have been used for a larger source follower and the select transistor. Another pixel configuration to utilize the space better could have been explored. Designing a bigger pixel that contains four pixels instead of a single pixel would make it possible to create more space efficient configurations. Moving the photodiodes to the corners would combine the unused space and make it more useable, and make it possible to increase transistor sizes.

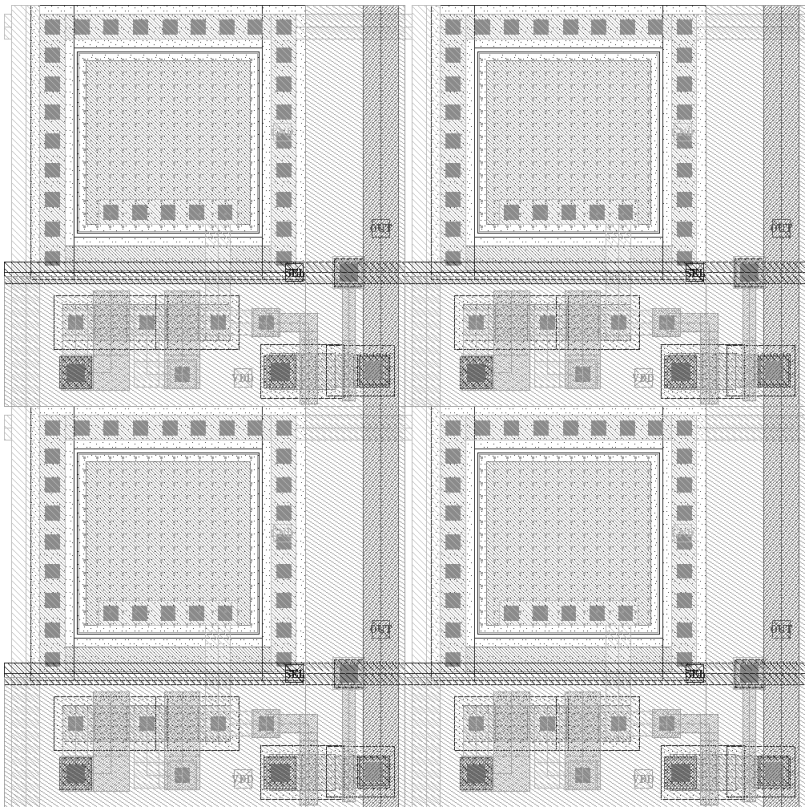

Figure 3.2: Layout of 4 pixel array.

3.3 Column amplifier

The column amplifier module contains a current source, a source follower and a column select transistor. The current source has a length of 10μm and width of 5μm and the column amplifier module has the size of 11.25μmx20μm, and the layout of a single column amplifier is shown in Figure 3.3. The width of the pixel limits the width of the column amplifier to 11.25μm. The wire for bias voltage runs horizontally across the bottom of the column amplifier and is connected to the gate of the current source which is placed at the bottom of every column amplifier module. The pixel column is connected to the drain of the current source and the gate of the source follower. The pMOS column select transistor is connected to the pMOS source follower. Four column amplifier modules are shown in Figure 3.4. This figure shows how the biasing wire and output wire runs horizontally through the column amplifiers. The bottom of the pixel column is connected to the top of the column amplifier and connects to the gate of the pMOS source follower and drain of the current source transistor located at the bottom of the column amplifier. The select signal is provided by the column decoder and runs from the gate of the select transistor and down on the left side of the current source transistor.

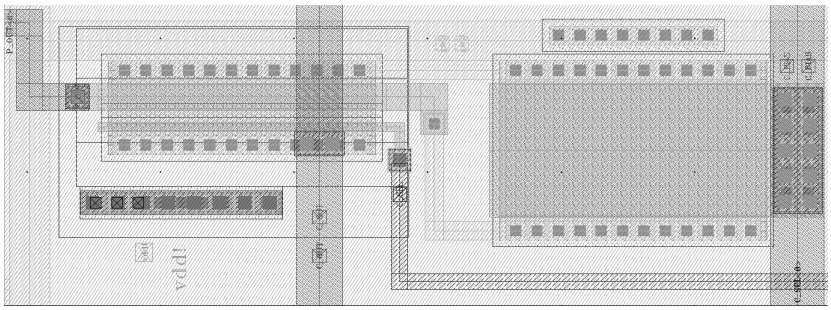

Figure 3.3: Layout of current source used, placed at the bottom of every pixel columns. Schematic shown in Figure 2.14. Figure has been rotated 90 degrees to the left. The current source is the large transistor shown on the right. The select and source follower is on the left

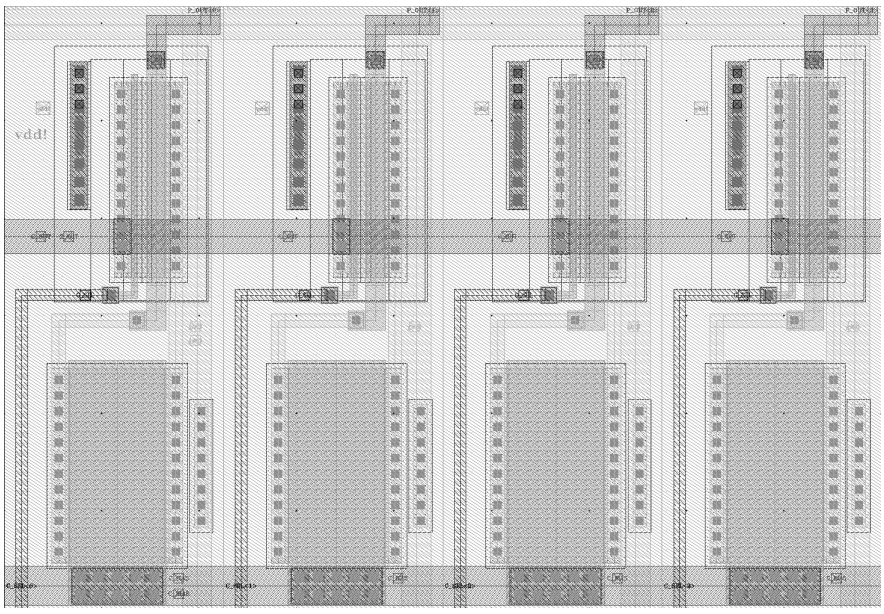

Figure 3.4: Layout showing four of the current sources placed at the bottom of four columns.

3.4 Decoder

The column decoder is designed for the pMOS select transistor in the column amplifier and has an active low operation. Part of the column decoder is shown in Figure 3.5, and is fundamentally identical to the row decoder. The row decoder, on the other hand, has an active high operation because of the nMOS select transistors, which is opposite to the column decoder. Active high operation with the same decoder is achieved by adding an inverter on every output as shown in Figure 3.6. The output lines pitch is 11.25μm to match the pixel pitch. The seven inputs for the decoder are connected to digital pads on the pad frame. This decoder is described more thoroughly in Soman Cheng's, Mathias Wilhelmsen's and Stian Hjorteset's master thesis [25][26][28].

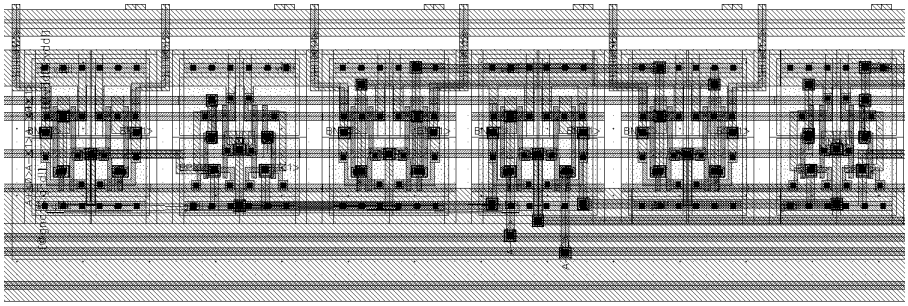

Figure 3.5: Layout of part of the column decoder.

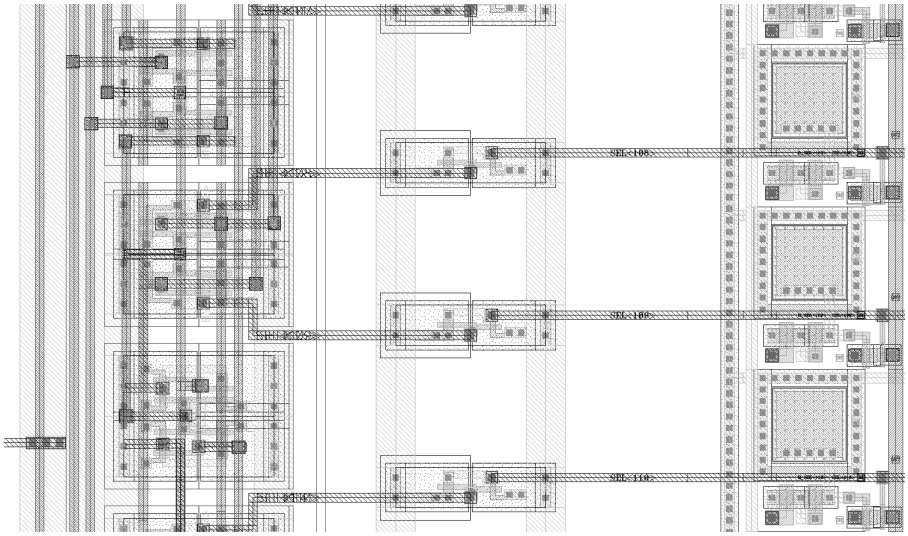

Figure 3.6: Layout of part of the row decoder.

3.5 Readout

Figure 3.7 shows the readout circuitry for the image sensor. The large component on the right is the output buffer provided by Philipp Hafliger.

The large pMOS transistor in the middle is a current source for the output line. The column on the left shows how the bottom of the pixel array is connected to the column amplifier module. The horizontal output wire can be seen running through the column amplifier and the current source to the output buffer.

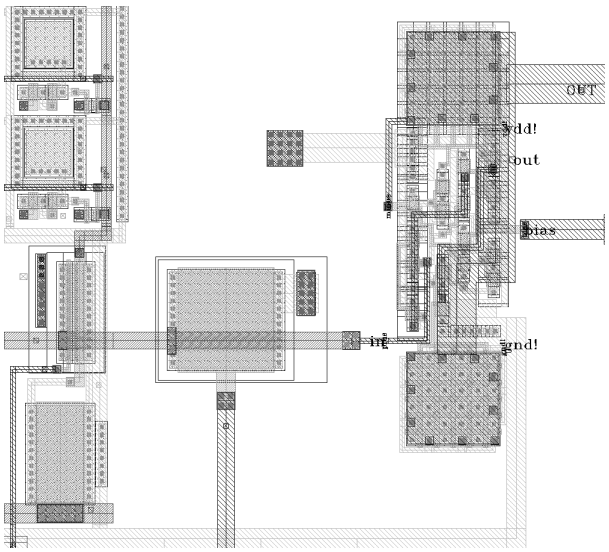

Figure 3.7: Layout of the corner showing pixel array column amplifier and readout.

3.6 Testability

Three extra photodiodes and a pixel were added for testing. The first test photodiode is shown in Figure 3.8. This is the same photodiode used in the pixel that is connected to a pad. Below this there is another test photodiode shown in Figure 3.9. Figure 3.10 shows a single pixel with a readout circuit that is identical to the full pixel array. The third photodiode is placed in the bottom right corner and is shown in Figure 3.11.

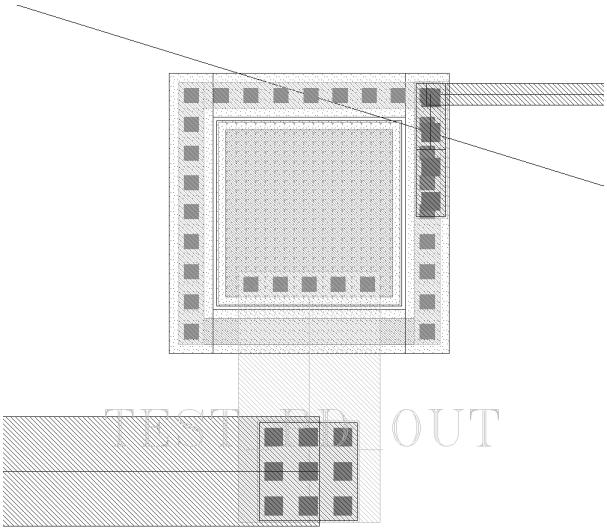

Figure 3.8: Layout of top left test pd layout

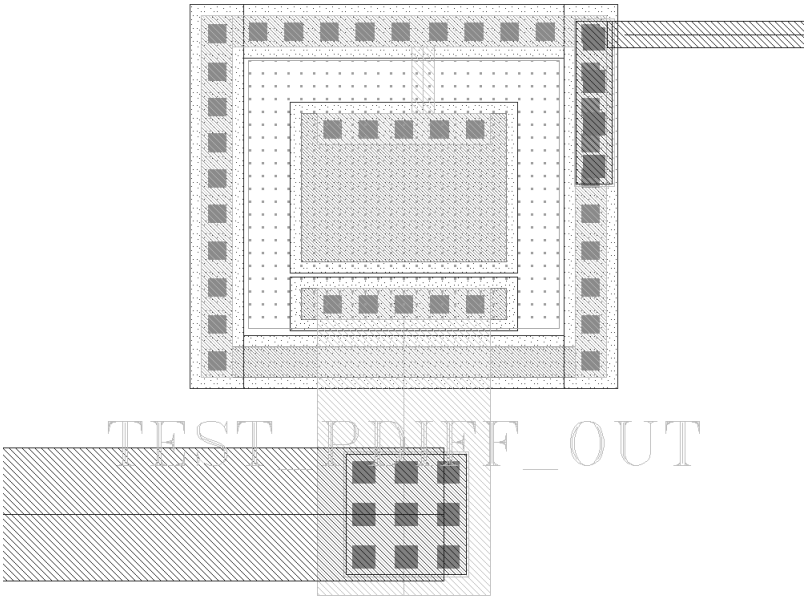

Figure 3.9: Layout of one of the test photodiodes.

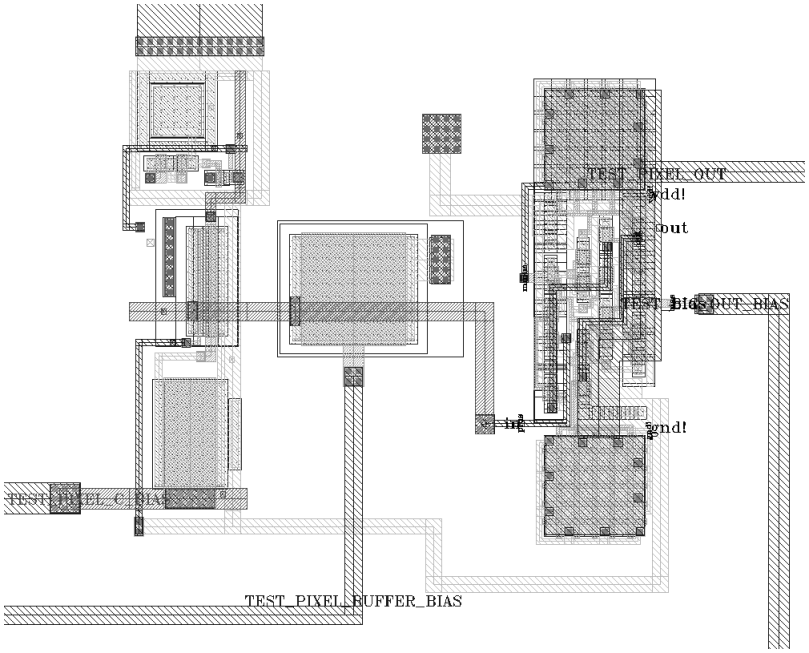

Figure 3.10: Layout of bottom pixel, which functions as a single pixel image sensor.

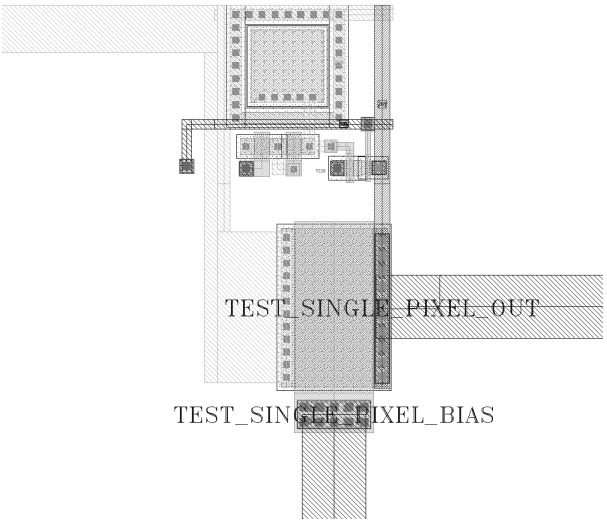

Figure 3.11: Layout of test pixel

3.7 Chip

The layout of the entire design is shown in Figure 3.12. This Figure shows the image sensor in the bottom left corner surrounded by decoupling capacitors. Other students use the blank space on the other side of the decoupling capacitors for their designs. The pad frame consists of 100 pads, divided into VDD pads, ground pads, analog pads, and digital pads. The entire image sensor, decoders and the area around is covered with Metal 4 and is used for VDD. Metal 4 is divided into digital and analog zones, where the metal 4 above the pixel array and column amplifier is used as the analog VDD. Metal 4 above the decoders is used for digital VDD. These VDD have dedicated pads on the pad frame for analog and digital VDD I/O.

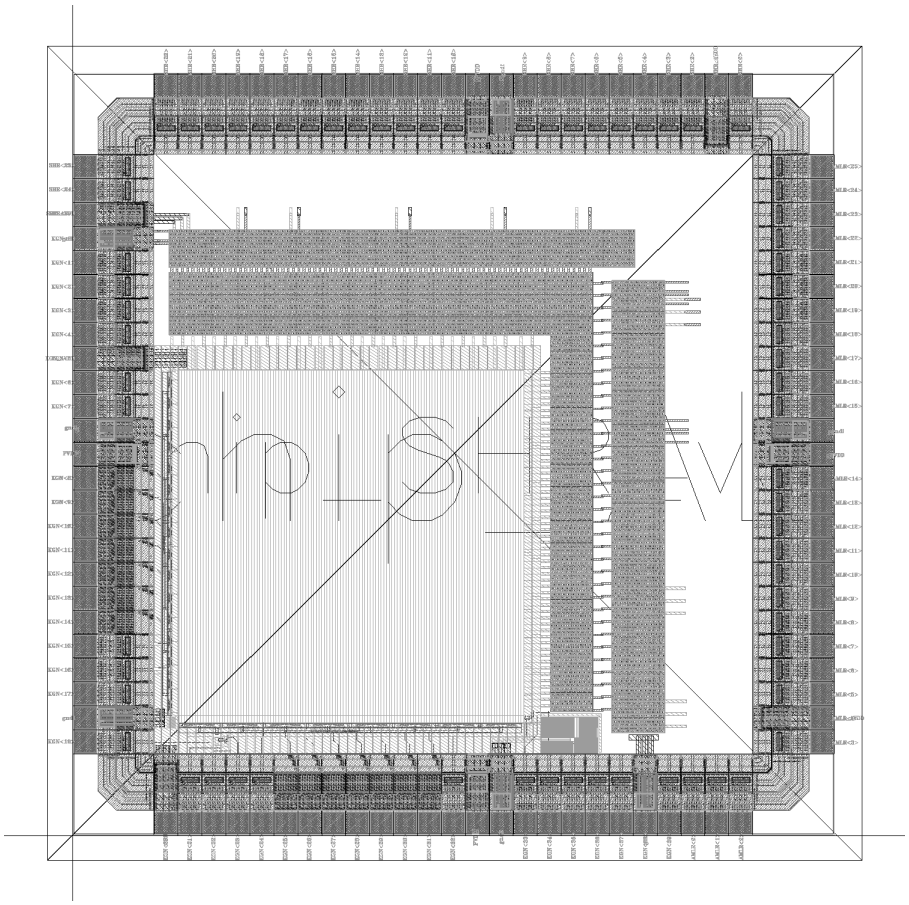

Figure 3.12: Full chip layout showing the image sensor and the pad frame. The chip has $2.5x2.5\mu$m of usable area.

Chapter 4

Printed circuit board

4.1 Schematic

The printed circuit board (PCB) consists of the image sensor, voltage regulator IC, USB connector, potentiometers, test pins and a lot of decoupling capacitors. Schematic of the PCB is shown in Figure 4.2. Bias voltages are set using a potentiometer connected between VDD and GND. Bias inputs and supply inputs have three decoupling capacitors connected in parallel. The PCB presented in this chapter is a preliminary design and is subject to change, as it was not sent to production before the deadline of this thesis.

4.2 Image sensor

The image sensor is mounted in a 100 pin package as shown in Figure 4.1. The layout for the package was provided by Mozhdeh Nematzadeh. Since the image sensor is placed at the bottom left corner, the pads allocated for the image sensor is the ones on the left and bottom side of the pad frame. The pads on the top and right side are allocated to the two other students' design. Not every pad allocated to the image sensor has been used. Table of the pins is shown in Table 4.1. VDD for the image sensor is 3.3V, and the image sensor has pads for both digital and analog VDD, which will be provided by the board. The boards VDD will be considered as the analog supply. To isolate the analog supply from the digital noise a small impedance and decoupling capacitors are added between the analog supply and digital VDD. The package for the image sensor is a ball grid array, which requires the use of multiple layers in the PCB. A lens will be fitted to the image sensor to focus the light onto the image sensor.

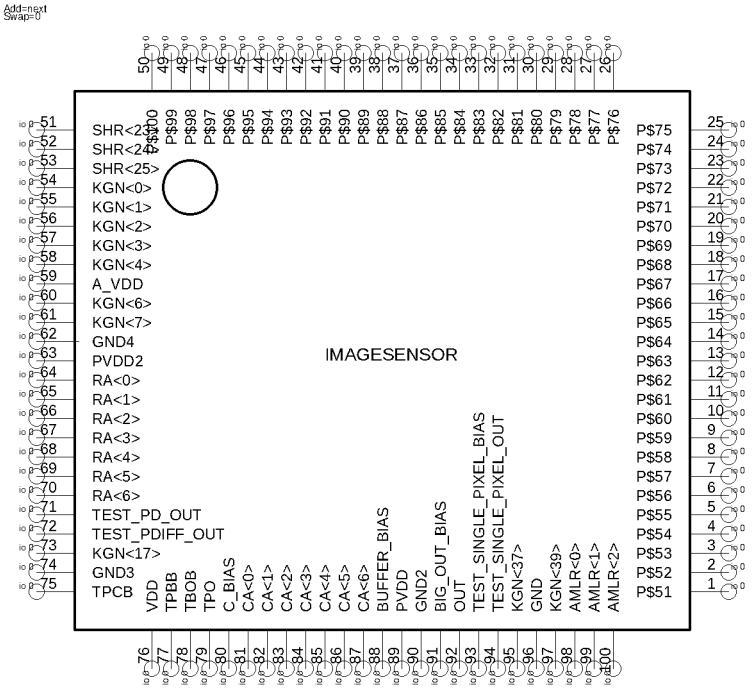

Figure 4.1: Symbol for the image sensor.

Pin	I/O	Description
A_VDD	Input/Output	VDD for the analog circuitry
GND4	Input/Output	GND
PVDD2	Input/Output	VDD for pad frame
RA<0..6>	Input	Digital input for row decoder
TEST_PD_OUT	Output	Output for the upper left test PD
TEST_PDIFF_OUT	Outout	Output for the lower left test PD
GND3	Input/Output	GND
TPCB	Input	Test pixel column bias
VDD	Input/Output	Digital VDD
TPBB	Input	Test pixel buffer bias
TBOB	Input	Test pixel output bias
TPO	Output	Test pixel output
C_BIAS	Input	Column bias
CA<0..6>	Input	Digital input for column decoder
BUFFER_BIAS	Input	Bias for the column current source
PVDD	Input/Output	VDD for pad frame
GND2	Input/Output	GND for pad frame
BIG_OUT_BIAS	Input	Bias for the output buffer
OUT	Output	Output for the image sensor
TEST_SINGLE_PIXEL_BIAS	Input	Input for single pixel bias
TEST_SINGLE_PIXEL_OUT	Input	Input for single pixel out
GND	Input/Output	GND

Table 4.1: Overview of pins for the chip

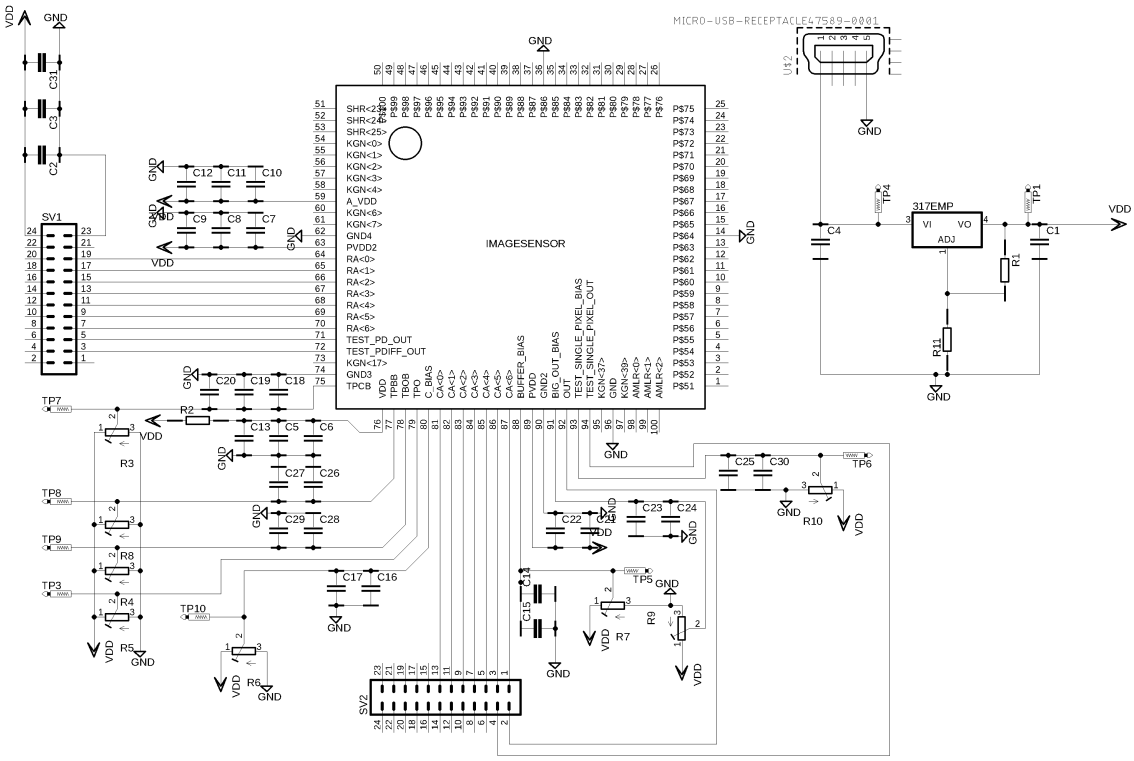

Figure 4.2: Schematic of the PCB.

4.3 FPGA

A zedboard development board will be used for controlling this image sensor. The zedboard has an FPGA and an ADC that will be used for the output signals. The FPGA will be used to provide column and row address for both image capture mode and for the pixel that is going to receive optical communication signals. The operation for the FPGA is first to capture an image. The FPGA has to provide address' for every pixel, read the value, convert the analog signal to digital with the onboard ADC, and then store the digital value with its address in memory. After the image have been captured and stored, the spatial coordinates for the pixel that contains the light source must be extracted. Spatial coordinates can be extracted with software that can recognize the light source, or in this case, be manually extracted from the image. After the spatial coordinates have been extracted, it can then be inputted to the FPGA with the eight switches on the board.

4.4 Layout

Since this PCB contains a mixed signal IC, some extra considerations have to be made. The board will have a single ground plane used for both digital and analog circuit. This is to prevent ground loops or non-optimal return current paths. Using a single ground plane requires that the PCB

is partitioned into digital and analog sections. The digital power line will be routed as a signal wire from the analog power plane to the small resistor and decoupling capacitors then to the digital VDD pin. Decoupling capacitors should be placed as close as possible to the IC.

Chapter 5

Discussion

The image sensor in this project can only either capture an image or receive, this is because the image sensor has only one output line. Adding dedicated output circuitry that contains amplifier and comparator that has low capacitance and designed for high-speed VLC might increase the bandwidth. Another aspect is receiving from multiple sources. This requires additional outputs for parallel optical reception.

A single pixel topology image sensor for VLC has the advantage over the dual topology pixel image sensor that it uses less area. A pixel array with the same resolution as the dual pixel topology solution will be smaller and more pixels or signal processing circuits can be fitted on the same area. Additionally, the use of logarithmic pixels can provide high dynamic range images for machine vision and safety applications.

One significant aspect of V2V-VLC is real-time tracking of the transmitting light sources. This aspect has not been explored in this project. In automotive applications, the light source will be on a spatially fixed position when the vehicle is stationary. For a moving vehicle, real-time tracking is needed to track the transmitting light source and at the same time maintain an unbroken connection when the light source moves spatially. This can be done with signal processing. However, doing it with signal processing might not be fast enough. Without a good tracking system, V2V-VLC will be challenging. Earlier it has been done by using a pixel array with alternating pixel topologies with dedicated hardware for real-time tracking [8].

Bandwidth is something that depends on many factors such as wavelength, lumens of the incident light and the semiconductor material. According to simulations the bandwidth is limited by the photodiode. In high-speed optical communication, high bandwidth can be achieved by using a transimpedance amplifier and an equalizer to extend the bandwidth across Gbit/s range. However, using transimpedance amplifier and equalizer have not been studied in this thesis, and could be difficult to implement.

Chapter 6

Future work

The future work for this project is to finish the PCB and test the image sensor when it arrives. The goal is to get this into a working system that has the capability for live data transfer, to transmit live video or audio through the image sensor. To achieve this, a demodulation circuit must be implemented for live reception of data. However, the priority is to confirm 1MHz reception with the use of an oscilloscope. The production of the image sensor was delayed, the image sensor could not be tested, and receiving capability could not be determined.

Also, a modulation circuit to transmit modulated data with a LED has to be designed. The frequency and optical output should be adjustable to measure bandwidth in a different condition, optical power, and frequencies. Control system and software to capture an image needs to be created, this is required to find which pixel corresponds to the spatial location of the LED light source. Adapting the software created by previous students might be possible. The software should search for a light source in the captured image to get the spatial address. When the spatial address is available, the software can start optical transmission.

Modulation techniques and encodings have not been explored in this project and could be looked into. The photodiode can be optimized further to increase bandwidth. Different photodiodes and pixel topologies for optimized optical reception and still image capturing could be explored.

An image sensor using the emerging 3D technology can have the image sensor and analog circuit on one level, and the digital circuits on another level. This opens up the possibility to add transimpedance amplifier and equalizer circuit to extend the bandwidth into the hundreds of Mbit/s.

5G is an emerging cellular mobile communication and has many benefits over the current 4G technology. The biggest advantage is higher bitrate and significantly lower latency [29]. V2V can be used for identification and establish a 5G WLAN between vehicles and infrastructure quickly. With 5G technology, it is possible to wirelessly transmit data with very low latency.

The test photodiodes can be tested with a transimpedance amplifier and equalizer circuit, to test if bandwidth in the hundreds of megabits is possible or even a gigahertz. It can also be used to measure the amount of photocurrent the photodiode generates for different conditions.

Chapter 7

Conclusion

A single-pixel topology CMOS image sensor for visible light communication has been designed and produced. Due to a production delay at the manufacturer, the image sensor was not delivered in time for testing. Simulations show that a bandwidth of 1MHz is achievable. The log pixels can provide high dynamic range video for light source detection and safety features for automotive applications. VLC and DSRC give autonomous vehicles a way to connect to nearby vehicles and infrastructure, and I believe this technology will be part of the future of ITS.

Bibliography

[1] T. Komine and M. Nakagawa. "Fundamental analysis for visible-light communication system using LED lights". In: *IEEE Transactions on Consumer Electronics* 50.1 (Feb. 2004), pp. 100–107. ISSN: 0098-3063. DOI: 10.1109/TCE.2004.1277847.

[2] Shlomi Arnon. *Visible Light Communication*. Cambridge University Press, 2015. ISBN: 978-1-107-06155-2.

[3] D. Karunatilaka et al. "LED Based Indoor Visible Light Communications: State of the Art". In: *IEEE Communications Surveys Tutorials* 17.3 (2015), pp. 1649–1678. ISSN: 1553-877X. DOI: 10.1109/COMST.2015.2417576.

[4] J Ely. "Electromagnetic Interference to Flight Navigation and Communication Systems: New Strategies in the Age of Wireless". In: (Aug. 2005). DOI: 10.2514/6.2005-6361.

[5] Latif Ullah Khan. "Visible light communication: Applications, architecture, standardization and research challenges". In: *Digital Communications and Networks* 3.2 (2017), pp. 78–88. ISSN: 2352-8648. DOI: https://doi.org/10.1016/j.dcan.2016.07.004. URL: http://www.sciencedirect.com/science/article/pii/S2352864816300335.

[6] Eun Tae Won et al. *Visible Light Communication : Tutorial*. http://www.ieee802.org/802_tutorials/2008-03/15-08-0114-02-0000-VLC_Tutorial_MCO_Samsung-VLCC-Oxford_2008-03-17.pdf. [Online; accessed 10-May-2018]. 2008.

[7] World Health Organization. *Road traffic injuries*. http://www.who.int/mediacentre/factsheets/fs358/en/. [Online; accessed 10-April-2018]. 2018.

[8] T. Yamazato et al. "Image-sensor-based visible light communication for automotive applications". In: *IEEE Communications Magazine* 52.7 (July 2014), pp. 88–97. ISSN: 0163-6804. DOI: 10.1109/MCOM.2014.6852088.

[9] I. E. Lee, M. L. Sim, and F. W. L. Kung. "Performance enhancement of outdoor visible-light communication system using selective combining receiver". In: *IET Optoelectronics* 3.1 (Feb. 2009), pp. 30–39. ISSN: 1751-8768. DOI: 10.1049/iet-opt:20070014.

[10] Hugh Sing Liu and G. Pang. "Positioning beacon system using digital camera and LEDs". In: *IEEE Transactions on Vehicular Technology* 52.2 (Mar. 2003), pp. 406–419. ISSN: 0018-9545. DOI: 10.1109/TVT.2003.808800.

[11] Filip Tavernier and Michiel Steyaert. *High-Speed Optical Receivers with Integrated Photodiode in Nanoscale CMOS*. Springer, 2011. ISBN: 978-1-4419-9924-5.

[12] Umesh K. Mishra and Jasprit Singh. *Semiconductor Device Physics and Design*. Springer, 2008. ISBN: ISBN 978-1-4020-6480-7.

[13] K. Murari et al. "Which Photodiode to Use: A Comparison of CMOS-Compatible Structures". In: *IEEE Sensors Journal* 9.7 (July 2009), pp. 752–760. ISSN: 1530-437X. DOI: 10.1109/JSEN.2009.2021805.

[14] N. Teranishi. "Effect and Limitation of Pinned Photodiode". In: *IEEE Transactions on Electron Devices* 63.1 (Jan. 2016), pp. 10–15. ISSN: 0018-9383. DOI: 10.1109/TED.2015.2433532.

[15] H. Amhaz and G. Sicard. "A high output voltage swing logarithmic image sensor designed with on chip FPN reduction". In: *6th Conference on Ph.D. Research in Microelectronics Electronics*. July 2010, pp. 1–4.

[16] W. Chou et al. "A Linear-Logarithmic CMOS Image Sensor With Pixel-FPN Reduction and Tunable Response Curve". In: *IEEE Sensors Journal* 14.5 (May 2014), pp. 1625–1632. ISSN: 1530-437X. DOI: 10.1109/JSEN.2013.2294740.

[17] F. de Souza Campos et al. "A logarithmic CMOS image sensor with wide output voltage swing range". In: *2017 International Caribbean Conference on Devices, Circuits and Systems (ICCDCS)*. June 2017, pp. 69–72. DOI: 10.1109/ICCDCS.2017.7959722.

[18] S. Kavadias et al. "A logarithmic response CMOS image sensor with on-chip calibration". In: *IEEE Journal of Solid-State Circuits* 35.8 (Aug. 2000), pp. 1146–1152. ISSN: 0018-9200. DOI: 10.1109/4.859503.

[19] I. Takai et al. "LED and CMOS Image Sensor Based Optical Wireless Communication System for Automotive Applications". In: *IEEE Photonics Journal* 5.5 (Oct. 2013), pp. 6801418–6801418. ISSN: 1943-0655. DOI: 10.1109/JPHOT.2013.2277881.

[20] https://www.uio.no/studier/emner/matnat/ifi/INF5442/h17/timeplan/inf5442_h17_3_ch3_noise_20sep2017.pdf. 2017.

[21] Junichi Nakamura. *Image sensors and signal processing for digital still cameras*. CRC Press, 2006. ISBN: 0-8493-3545-0.

[22] R. H. Nixon et al. "256/spl times/256 CMOS active pixel sensor camera-on-a-chip". In: *IEEE Journal of Solid-State Circuits* 31.12 (Dec. 1996), pp. 2046–2050. ISSN: 0018-9200. DOI: 10.1109/4.545830.

[23] *Key differences between rolling shutter and frame (global) shutter*. https://eu.ptgrey.com/KB/10028. 2015.

[24] A. Krymski. "Implementing global shutter in a 4T pixel". In: *International image sensor workshop* (2009). URL: http://www.imagesensors.org/Past%5C%20Workshops/2009%5C%20Workshop/2009%5C%20Papers/077_paper_krymski_gs.pdf.

[25] Soman Cheng. *Design and test of a 128x128 Pixel Global Shutter CIS with HDR Support*. http://urn.nb.no/URN:NBN:no-59607. 2017.

[26] Mathias Wilhelmsen. *Design of CMOS Image Sensor with Linear Readout Amplifier*. http://urn.nb.no/URN:NBN:no-57208. 2016.

[27] Marius Lunder Lillestøl. *Design and test of a CMOS image sensor with global shutter and High Dynamic Range*. http://urn.nb.no/URN:NBN:no-59606. 2017.

[28] Stian Hjorteset. *Design of CMOS image sensor with high linear amplifier*. http://urn.nb.no/URN:NBN:no-57754. 2016.

[29] GSMA Intelligance. *Understanding 5G: Perspectives on future technological advancements in mobile*. https://www.gsmaintelligence.com/research/?file=141208-5g.pdf&download. [Online; accessed 30-April-2019]. 2014.